

FLUID-STRUCTURE INTERACTION IN A PRE-STRESSED TUBE WITH THICK ELASTIC WALLS I: THE STATIONARY STOKES PROBLEM

ANDRO MIKELIĆ, GIOVANNA GUIDOBONI, SUNČICA ČANIĆ

(Communicated by Aim Sciences)

ABSTRACT. This is a study of the fluid-structure interaction between the stationary Stokes flow of an incompressible, Newtonian viscous fluid filling a three-dimensional, linearly elastic, pre-stressed hollow tube. The main motivation comes from the study of blood flow in human arteries. Most literature on fluid-structure interaction in blood flow utilizes thin structure models (shell or membrane) to describe the behavior of arterial walls. However, arterial walls are thick, three-dimensional structures with the wall thickness comparable to the vessel inner radius. In addition, arteries *in vivo* exhibit residual stress: when cut along the radius, arteries spring open releasing the residual strain. This work focuses on the implications of the two phenomena on the solution of the fluid-structure interaction problem, in the parameter regime corresponding to the blood flow in medium-to-large human arteries. In particular, it is assumed that the aspect ratio of the cylindrical structure $\epsilon = R/L$ is small. Using asymptotic analysis and ideas from homogenization theory for porous media flows, an effective, closed model is obtained in the limit as both the thickness of the vessel wall and the radius of the cylinder approach zero, simultaneously. The effective model satisfies the original three-dimensional, axially symmetric problem to the ϵ^2 -accuracy. Several novel properties of the solution are obtained using this approach. A modification of the well-known “Law of Laplace” is derived, holding for thick elastic cylinders. A calculation of the effective longitudinal displacement is obtained, showing that the leading-order longitudinal displacement is completely determined by the external loading. Finally, it is shown that the residual stress influences the solution only at the ϵ -order. More precisely, it is shown that the only place where the residual stress influences the solution of this fluid-structure interaction problem is in the calculation of the ϵ -correction of the longitudinal displacement.

1. Introduction. The focus of this paper is on the fluid-structure interaction between a viscous, incompressible, Newtonian fluid flowing through a pre-stressed tube with thick, three-dimensional elastic walls. The main motivation comes from

2000 *Mathematics Subject Classification.* Primary: 35Q30, 74K15; Secondary: 76D27.

Key words and phrases. Fluid-structure Interaction, Three-Dimensional Elastic Walls, Blood Flow, Compliant Tube.

The first author is affiliated with Université de Lyon, Lyon, F-69003, France; Université Lyon 1, Institut Camille Jordan, UFR Mathématiques, Site de Gerland, Bat. A, 50, avenue Tony Garnier, 69367 Lyon Cedex 07, FRANCE. The second and the third authors are affiliated with the Department of Mathematics, University of Houston, Houston, Texas 77204-3476.

the study of blood flow in human arteries. In the last few years there has been a significant growth in interest in the theoretical and numerical study of fluid-structure interaction problems arising in blood flow. This is a complex problem involving several spatial and temporal scales, and a severe nonlinearity in the coupling between the fluid and the structure (vessel wall). In addition, vessel walls are anisotropic and inhomogeneous, composed of several layers with different mechanical properties. Taking into account the detailed mechanical structure of the arterial walls would make the study of the fluid-structure interaction intractable. This is why most models in the related literature utilize the simple linearly elastic (or viscoelastic) membrane equations to model the behavior of arterial walls, see [1, 3, 4, 6, 7, 15, 16, 21, 22, 23, 24]. In particular, the membrane models assume small vessel wall thickness with respect to the vessel inner radius (lumen). This is, however, not the case in the blood flow application. Arterial walls are **thick** three-dimensional structures, with the vessel wall thickness h comparable to the vessel inner radius R (lumen), [20]. See Figure 1. The focus of this paper is on the fluid-structure interaction between a viscous, incompressible, Newtonian fluid flowing through a pre-stressed tube with thick, three-dimensional elastic walls. The main motivation comes from the study of blood flow in human arteries. In the last few years there has been a significant growth in interest in the theoretical and numerical study of fluid-structure interaction problems arising in blood flow. This is a complex problem involving several spatial and temporal scales, and a severe nonlinearity in the coupling between the fluid and the structure (vessel wall). In addition, vessel walls are anisotropic and inhomogeneous, composed of several layers with different mechanical properties. Taking into account the detailed mechanical structure of the arterial walls would make the study of the fluid-structure interaction intractable. This is why most models in the related literature utilize the simple linearly elastic (or viscoelastic) membrane equations to model the behavior of arterial walls, see [1, 3, 4, 6, 7, 15, 16, 21, 22, 23, 24]. In particular, the membrane models assume small vessel wall thickness with respect to the vessel inner radius (lumen). This is, however, not the case in the blood flow application. Arterial walls are **thick** three-dimensional structures, with the vessel wall thickness h comparable to the vessel inner radius R (lumen), [20]. See Figure 1. Taking this property into account leads to new information about the coupling between arterial walls and blood flow, discussed in detail in Sections 4.3 and 7. In particular, we arrive to a modification of the Law of Laplace that relates the fluid pressure with the wall displacement holding for thick walls.

Furthermore, most of the models used in the literature on the interaction between blood flow and vessel walls, do not account for the fact that arteries *in vivo* exhibit **residual stress**: if cut radially, arteries spring open releasing the residual strain and approaching the zero-stress state which is a sector, shown in Figures 3 and 4. See [9, 11, 16, 17, 18, 25]. In this manuscript we take both phenomena into account to derive a simple, effective closed model that approximates the three-dimensional axially symmetric problem to the ϵ^2 -accuracy, where $\epsilon = R/L \ll 1$ is the aspect ratio of the vessel segment of length L .

More precisely, we study the fluid-structure interaction problem between a **three-dimensional**, linearly elastic thick, **pre-stressed**, hollow tube filled with an incompressible, Newtonian viscous fluid satisfying the Stokes equations. Assuming the aspect ratio of the tube to be small, and letting the thickness of the tube wall to be of the same order of magnitude as the tube radius, we derive a closed

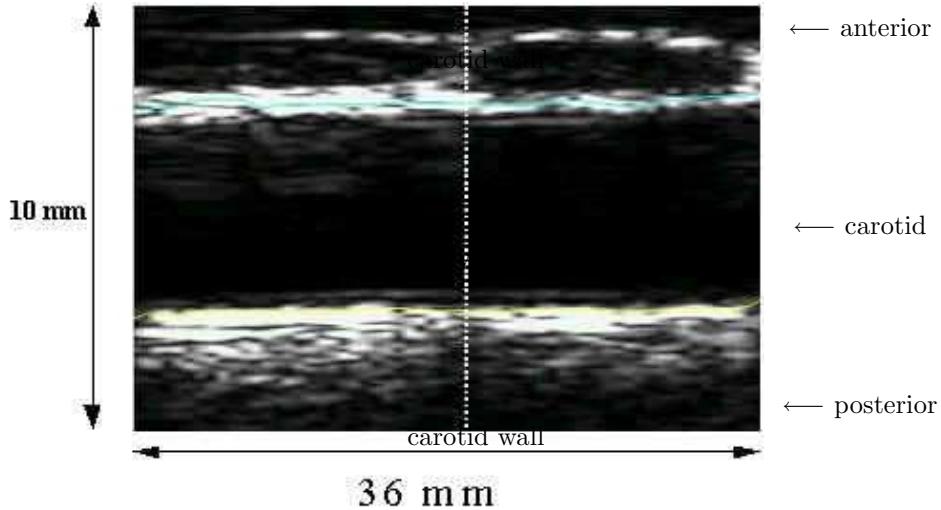


FIGURE 1. Ultrasound of the human carotid artery, [8].

effective model that approximates the three-dimensional axially symmetric problem to the ϵ^2 -accuracy. From the reduced model the following three interesting new results follow. One is a new algebraic relationship between the fluid pressure and the vessel radius for *thick* structures, given by (127), that is a modification of the well-known Law of Laplace that holds for thin membrane shells. This is obtained in Section 7. We show that using the classical Law of Laplace to study the pressure-displacement relationship for thick structures, under-estimates the radial displacement of the structure. In particular, the error increases with the thickness of the wall and is of order $O(1)$ for medium-to-large arteries. Thus, we suggest that using the pressure-radius relationship (127) is more appropriate for the blood-flow application. The second result concerns the influence of the residual stress on the solution of the fluid-structure interaction problem to the $O(\epsilon^2)$ accuracy. Residual stresses have been studied extensively in the past ten year in the context of modeling the mechanical properties of vessel walls. It has been shown using numerical simulations of the arterial wall mechanics, [17], that under the static physiological loading, the influence of the residual stress on the vessel wall displacement is relatively small. In this paper, we show using asymptotic analysis, that even though the residual stress does not enter the solution to the leading order accuracy, it influences the calculation of the longitudinal displacement of the vessel wall to the ϵ accuracy. This is shown in Section 6. And finally, our third result concerns the magnitude of the longitudinal displacement. Most of the literature on fluid-structure interaction in blood flow assumes that the longitudinal displacement of the vessel wall is zero, arguing that the vessel walls are longitudinally theatered, composed of a "series" of approximately independent rings giving rise to the negligible longitudinal displacement. In this manuscript we show in a consistent way that the

leading-order longitudinal displacement is zero, assuming that the longitudinal displacement of the cylinder's external boundary is zero. More precisely, we show that in *any* three-dimensional linearly elastic cylindrical tube that is interacting with an axially symmetric flow of an incompressible, viscous fluid, the leading-order longitudinal displacement in the three-dimensional structure is completely determined by the ambient boundary condition applied to the external lateral boundary of the cylinder. This result is a consequence of the fact that the axial component of the fluid stress at the fluid-structure interface is negligible to the leading order. Thus, if the external boundary of the vessel wall is longitudinally fixed, the longitudinal displacement throughout the three-dimensional cylindrical wall will remain zero to the leading-order accuracy. However, we also show that the ϵ -correction of the longitudinal displacement is not zero. In fact, the ϵ -correction of the longitudinal displacement depends on the residual stress, the tangential component of the fluid stress, and on the zero-th order approximation of the radial displacement. This is obtained in Section 4.3 and Section 5.

2. Mathematical formulation. We study the flow of an incompressible viscous fluid through a pre-stressed tube with three-dimensional linearly elastic walls of thickness h . The main assumptions in this paper are that the thickness h is comparable to the inner tube radius R which is small with respect to the tube length L :

$$\frac{h}{R} = O(1), \quad \frac{R}{L} = \epsilon,$$

and that the walls of the tube, prior to the physiological loading, exhibit non-zero residual stress.

It has been well accepted that blood in medium-to-large arteries can be modeled as a viscous, incompressible, Newtonian fluid, utilizing the Navier-Stokes equations as a good flow model. The study of the fluid-structure interaction between the incompressible, viscous Navier-Stokes equations and the equations of the three-dimensional, linearly elastic structure, is complicated due to the following features: the fluid equations are non-linear and the time-dependent coupling between the flow and the structure introduces additional nonlinearities in the problem. In particular, the time-scale at which the waves in the structure and the fluid flow are captured to the leading order accuracy, is determined by both the time scale of the "far field" velocity, as well as the time scale of the vibrations of the structure, see [7, 2]. However, in our current work, we have realized that in order to understand the influence of the residual stress and the structure's wall thickness on the solution to the fluid-structure interaction problem, it is sufficient to focus on the stationary Stokes problem, thereby avoiding additional difficulties associated with the time-dependent coupling. This is why in this paper, to keep ideas simple and to emphasize the basic features of the underlying fluid-structure interaction problem, we first focus on the stationary Stokes problem. The results presented here will still hold in the non-stationary Navier-Stokes case where additional difficulties related to the time-dependent coupling with a three-dimensional structure, will be dealt separately in [2].

For completeness, in this section we present the general, non-stationary fluid-structure interaction problem for the Navier-Stokes equations coupled with the three-dimensional structure equations, and focus on the stationary Stokes problem in the next section.

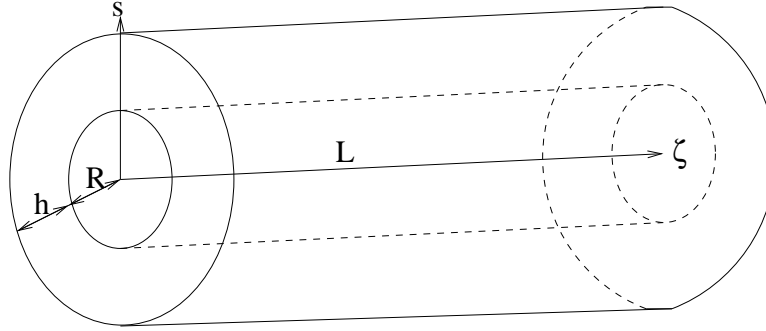


FIGURE 2. Prestressed reference configuration for a tube with three-dimensional elastic walls.

We begin by a description of the structure equations and the form of the Cauchy stress tensor describing residual stress due to the circumferential and longitudinal stretch. Since the structure equations are typically given in the Lagrangian framework (measuring the deformation of the structure with respect to a fixed reference configuration), and the flow equations are typically given in the Eulerian framework, we use different notation denoting the two coordinate systems: we will be using (r, θ, z) to denote the radial, azimuthal, and axial variable in the domain occupied by the fluid, and (s, ϑ, ζ) to measure the radial, azimuthal, and axial variable in the domain corresponding to the structure.

2.1. Description of the elastic structure. The reference configuration Ω_0^w for the elastic structure (wall) is a cylinder with annular cross section, with the internal and external radii R and $R+h$, respectively. See Figure 2.

In cylindrical coordinates the reference domain is given by

$$\Omega_0^w = \{(s \cos \vartheta, s \sin \vartheta, \zeta) \in \mathbf{R}^3 \mid s \in (\mathbf{R}, \mathbf{R} + \mathbf{h}), \vartheta \in [0, 2\pi), \zeta \in (0, \mathbf{L})\}, \quad (1)$$

with the exterior boundary

$$\Sigma_{\text{ext}}^w = \{(s \cos \vartheta, s \sin \vartheta, \zeta) \in \mathbf{R}^3 \mid s = \mathbf{R} + \mathbf{h}, \vartheta \in [0, 2\pi), \zeta \in (0, \mathbf{L})\}, \quad (2)$$

the interior boundary

$$\Sigma_{\text{int}}^w = \{(s \cos \vartheta, s \sin \vartheta, \zeta) \in \mathbf{R}^3 \mid s = \mathbf{R}, \vartheta \in [0, 2\pi), \zeta \in (0, \mathbf{L})\}, \quad (3)$$

and the inlet and outlet sections

$$\Sigma_0^w = \{(s \cos \vartheta, s \sin \vartheta, \zeta) \in \mathbf{R}^3 \mid s \in (\mathbf{R}, \mathbf{R} + \mathbf{h}), \vartheta \in [0, 2\pi), \zeta = 0\}, \quad (4)$$

$$\Sigma_L^w = \{(s \cos \vartheta, s \sin \vartheta, \zeta) \in \mathbf{R}^3 \mid s \in (\mathbf{R}, \mathbf{R} + \mathbf{h}), \vartheta \in [0, 2\pi), \zeta = \mathbf{L}\}. \quad (5)$$

We will be assuming that the reference configuration Ω_0^w is pre-stressed. Namely, it is well-known that arteries *in vivo* exhibit residual stress: when cut along the radius, an artery springs open to form an open sector, see Figures 3 and 4, [9, 17, 16]. Residual stress is the stress supported by a body in a fixed reference configuration in the absence of external forces, [18]. Residual stress is the Cauchy stress field \mathbf{T} satisfying the equilibrium equations and the zero traction condition, [18]:

$$\nabla \cdot \mathbf{T} = \mathbf{0} \quad \text{in } \Omega_0^w, \quad (6)$$

$$\mathbf{T}\mathbf{n} = \mathbf{0} \quad \text{on } \partial\Omega_0^w, \quad (7)$$

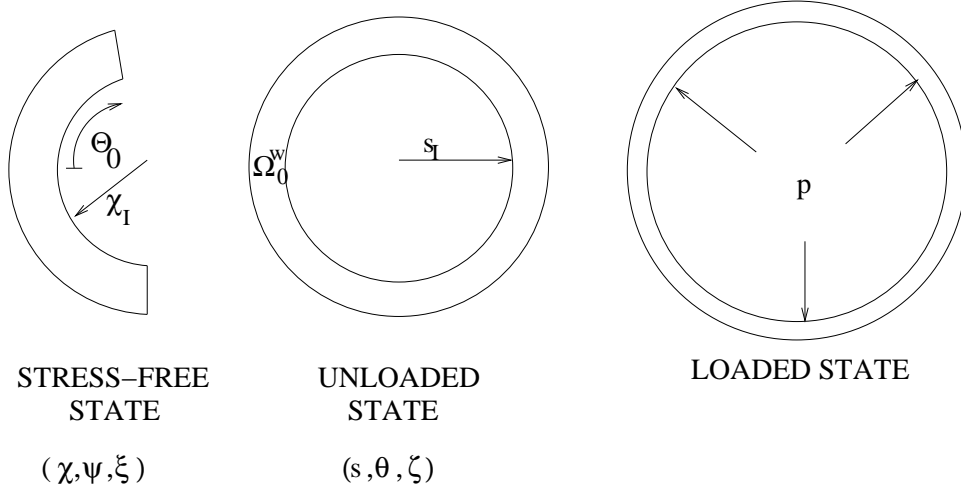


FIGURE 3. Cross-section of an arterial segment in the stress-free, unloaded and loaded state.

where \mathbf{n} is the outward unit normal. To calculate the distribution of residual stress, we used the approach and the results presented in [9, 11, 18, 17, 16]. In contrast with the rest of the manuscript where incremental elasticity is used to study the deformation from the pre-stressed, reference configuration Ω_0^w , the calculation of the residual stress relies on the theory of finite elasticity. A brief summary is presented next.

2.1.1. *The form of the Cauchy stress tensor for the residual stress due to the circumferential and longitudinal stretch.* Assume that the stress-free configuration of the arterial wall is a cylinder with a cross-section which is an open sector as shown in Figure 3, left. Consider a mapping which takes a material particle from its position (χ, ψ, ξ) in the open sector, to the new position (s, ϑ, ζ) in the intact unloaded (ring) configuration Ω_0^w shown in Figure 3 center, given by:

$$s = s(\chi), \quad \vartheta = \frac{\pi}{\Theta_0} \psi, \quad \zeta = \Lambda \xi, \quad (8)$$

where Θ_0 is the opening angle and Λ is the axial stretch ratio associated with the residual stress, [16].

Assume that the vessel walls are incompressible. Then the product $\lambda_1 \lambda_2 \lambda_3$ of the principal stretch ratios

$$\lambda_1 = \frac{\partial s}{\partial \chi}, \quad \lambda_2 = \frac{\pi}{\Theta_0} \frac{s}{\chi}, \quad \lambda_3 = \Lambda$$

must be equal to 1. This implies

$$s^2 - s_I^2 = \frac{\Theta_0}{\pi \Lambda} (\chi^2 - \chi_I^2), \quad (9)$$

where χ_I and s_I are the internal radii in the stress-free and the unloaded configuration, respectively. The deformation gradient \mathbf{J} and the right Cauchy-Green tensor

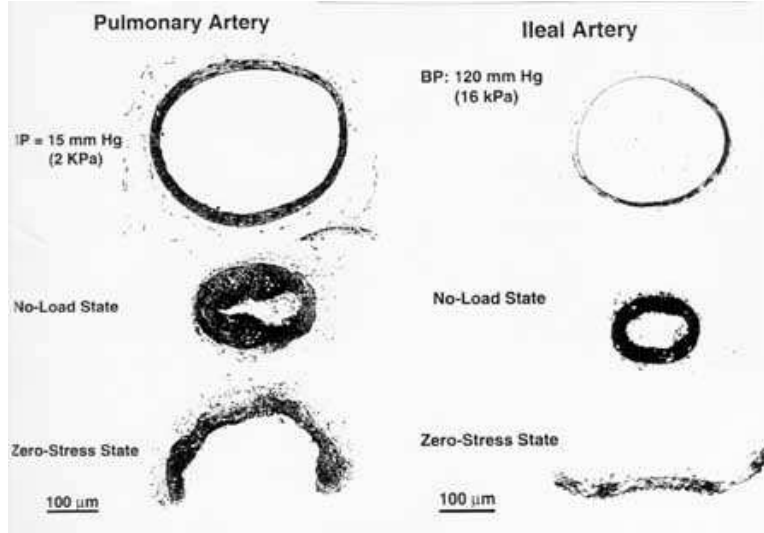


FIGURE 4. Residual Stress in Pulmonary and Ileal Artery, [25].

\mathbf{C} associated with this deformation, are given by the following, [16]:

$$\mathbf{J} = \begin{bmatrix} \frac{\Theta_0 \chi}{\pi \Lambda s} & 0 & 0 \\ 0 & \frac{\pi s}{\Theta_0 \chi} & 0 \\ 0 & 0 & \Lambda \end{bmatrix}, \quad \mathbf{C} = \begin{bmatrix} \left(\frac{\Theta_0 \chi}{\pi \Lambda s}\right)^2 & 0 & 0 \\ 0 & \left(\frac{\pi s}{\Theta_0 \chi}\right)^2 & 0 \\ 0 & 0 & \Lambda^2 \end{bmatrix}. \quad (10)$$

Define the Green-Lagrange strain tensor as $\mathbf{E} = (\mathbf{C} - \mathbf{I})/2$. Then, the Cauchy stress

<i>RESIDUAL STRESS PARAMETERS (CAROTID ARTERY) [11]</i>
$a = 44.2 \text{ kPa}$
$b = 16.7$
s_I (inner radius of the unloaded config.) = 3.1 mm
s_E (external radius of the unloaded config.) = 4.0 mm
χ_I (inner radius of the stress-free config.) = 5.05 mm
χ_E (external radius of the stress-free config.) = 6.04 mm

TABLE 1. Parameter values needed for the Residual Stress calculation

tensor can be obtained as follows, see [11]:

$$\mathbf{T} = p\mathbf{I} + \mathbf{J} \frac{\partial \Psi}{\partial \mathbf{E}} \mathbf{J}^T - \frac{1}{3} \left[\mathbf{J} \frac{\partial \Psi}{\partial \mathbf{E}} \mathbf{J}^T : \mathbf{I} \right] \mathbf{I}, \quad (11)$$

where p is the Lagrangian multiplier that ensures the incompressibility of the material, and Ψ is the strain-energy density function. In this manuscript we will be taking the strain-energy density function Ψ corresponding to the human carotid artery as proposed in [11]:

$$\Psi = \frac{a}{b} \left\{ \exp \left[\frac{b}{2} (I_1 - 3) \right] \right\}. \quad (12)$$

Here a and b are parameters representing the material properties and $I_1 := \mathbf{C} : \mathbf{I}$ is the first invariant of the right Cauchy-Green strain tensor \mathbf{C} . Substituting this expression into (11) we find that tensor \mathbf{T} depends only on the radial variable s and has a diagonal form with

$$T_{ss} = p + \frac{2}{3}\phi C_{ss}, \quad T_{\vartheta\vartheta} = p + \frac{2}{3}\phi C_{\vartheta\vartheta}, \quad T_{\zeta\zeta} = p + \frac{2}{3}\phi C_{\zeta\zeta}, \quad (13)$$

where

$$\phi = \frac{\partial\Psi}{\partial E_{ss}} = \frac{\partial\Psi}{\partial E_{\vartheta\vartheta}} = \frac{\partial\Psi}{\partial E_{\zeta\zeta}} = a \left\{ \exp \left[\frac{b}{2}(I_1 - 3) \right] \right\}, \quad (14)$$

and $C_{ss}, C_{\vartheta\vartheta}$ and $C_{\zeta\zeta}$ are the diagonal components of the Cauchy-Green stress tensor \mathbf{C} , given in (10). The zero traction condition implies $T_{ss}(R) = T_{ss}(R+h) = 0$. To calculate the Lagrange multiplier p we use the radial component of the equation $\nabla \cdot \mathbf{T} = \mathbf{0}$:

$$\frac{dT_{ss}}{ds} + \frac{T_{ss} - T_{\vartheta\vartheta}}{s} = 0. \quad (15)$$

Integrating equation (15) from the internal radius s_I to $s \in (R, R+h)$ one obtains

$$p = -\frac{2}{3}(\phi C_{ss} - L(s)), \quad \text{where } L(s) = \int_{s_I}^s \frac{\phi}{s} \left[\left(\frac{\Theta_0 \chi}{\pi \Lambda s} \right)^2 - \left(\frac{\pi s}{\Theta_0 \chi} \right)^2 \right] ds. \quad (16)$$

Using (11) we can now obtain the components of the Cauchy stress tensor describing the residual stress:

$$\boxed{T_{ss} = -\frac{2}{3}L(s), \quad T_{\vartheta\vartheta} = \frac{2}{3}[\phi(C_{\vartheta\vartheta} - C_{ss}) - L(s)], \quad T_{\zeta\zeta} = \frac{2}{3}[\phi(C_{\zeta\zeta} - C_{ss}) - L(s)],} \quad (17)$$

where $L(s)$ is defined in (16), ϕ in (14), and \mathbf{C} is the right Cauchy-Green tensor given by (10).

To completely specify the residual stress tensor we will be using parameter values from [11], shown in Table 1. The values for χ_I and χ_E are obtained by integrating equation (15) from s_I to s_E to get

$$\int_{s_I}^{s_E} \frac{\phi}{s} \left[\left(\frac{\Theta_0 \chi}{\pi \Lambda s} \right)^2 - \left(\frac{\pi s}{\Theta_0 \chi} \right)^2 \right] ds = 0. \quad (18)$$

Equation (18) is a compatibility condition. The choice of χ_I and χ_E must be such that (18) holds. In particular, we used $\chi_I = 5.05$ mm and $\chi_E = 6.04$ mm, and for the values of parameters Λ and Θ_0 we used the suggested values from [11, 16] which are $\Lambda = 1.1$ and $\Theta_0 = 0.638\pi = (1 - 130/360)\pi$.

Figures 5 and 6 show the components of the Cauchy stress tensor and the Green-Lagrange strain tensor plotted as a function of the radius. We can see that the magnitude of the radial component of the stress is much smaller than the circumferential and longitudinal ones, see Figure 5 left. Moreover, Figure 6 middle shows that the circumferential strain is negative in the inner part of the wall and positive in the outer part. This is in correspondence with the results in [18] and the experimental measurements presented in [9] and [16].

2.1.2. The Model Equations for the Structure. We assume that the elastic solid undergoes small deformations from the reference pre-stressed, unloaded configuration Ω_0^W , and that the gradient of the displacement $\mathbf{u} = (u_s, u_\vartheta, u_\zeta)$ from the reference configuration, $\nabla \mathbf{u}$, is small, allowing the use of linear theory. The equations of the

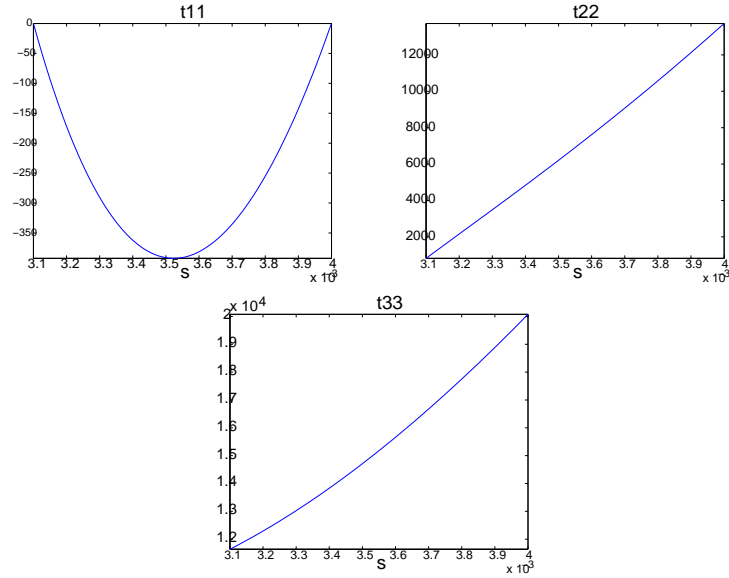


FIGURE 5. Diagonal components of the Cauchy stress tensor describing the residual stress.

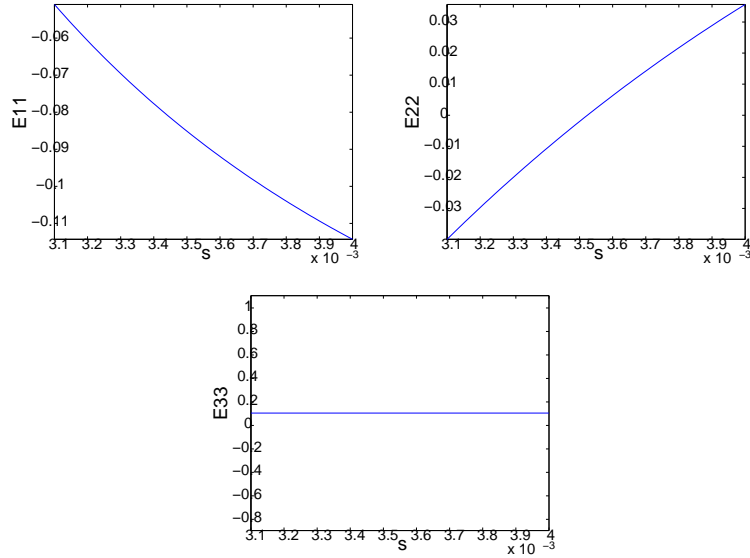


FIGURE 6. Diagonal components of the Green-Lagrange strain tensor describing the residual strains.

structure dynamics in the absence of body forces in the Lagrangian framework read as follows [18]:

$$\varrho_w \frac{\partial^2 \mathbf{u}}{\partial t^2} = \nabla \cdot \mathbf{S} \quad \text{in } \Omega_0^w, \quad (19)$$

where \mathbf{S} is the first Piola-Kirchhoff stress tensor. Following the approach in [18], we assume that \mathbf{S} is differentiable and that for small $\nabla \mathbf{u}$ it can be expressed as

$$\mathbf{S}(\mathbf{I} + \nabla \mathbf{u}) = \mathbf{S}(\mathbf{I}) + D\mathbf{S}(\mathbf{I})\nabla \mathbf{u}, \quad (20)$$

where we denoted by $\mathbf{S}(\mathbf{x})$ the stress tensor corresponding to the deformation \mathbf{x} . In the above expression, $\mathbf{S}(\mathbf{I})$ represents the stress in the structure in the absence of deformation. Therefore $\mathbf{S}(\mathbf{I}) = \mathbf{T}$. Tensor \mathbf{T} does not depend on the displacement \mathbf{u} or its gradient. The form of $D\mathbf{S}(\mathbf{I})\nabla \mathbf{u}$ is discussed in [18] and it is given by

$$D\mathbf{S}(\mathbf{I})\nabla \mathbf{u} = \mathbf{W}\mathbf{T} + \frac{1}{2}(\mathbf{E}\mathbf{T} - \mathbf{T}\mathbf{E}) + \mathbf{L}, \quad (21)$$

where \mathbf{L} is the (incremental) elasticity tensor

$$\mathbf{L} = 2\mu_w \mathbf{E} + \lambda_w (\text{tr} \mathbf{E}) \mathbf{I}, \quad (22)$$

with \mathbf{E} and \mathbf{W} denoting the infinitesimal strain and infinitesimal rotation, respectively,

$$\mathbf{E} = \frac{1}{2}(\nabla \mathbf{u} + (\nabla \mathbf{u})^t), \quad \mathbf{W} = \frac{1}{2}(\nabla \mathbf{u} - (\nabla \mathbf{u})^t), \quad (23)$$

with constants μ_w and λ_w corresponding to the counterparts of the Lamé constants of the classical theory.

For simplicity, we now introduce tensor \mathbf{Q}

$$\mathbf{Q} = \mathbf{T} + \mathbf{W}\mathbf{T} + \frac{1}{2}(\mathbf{E}\mathbf{T} - \mathbf{T}\mathbf{E}) \quad (24)$$

which accounts for the contribution of the pre-stress, so that \mathbf{S} can be simply expressed as

$$\mathbf{S} = \mathbf{Q} + \mathbf{L}.$$

Written in components, (19) reads:

$$\begin{aligned} \varrho_w \frac{\partial^2 u_s}{\partial t^2} &= \frac{S_{ss} - S_{\vartheta\vartheta}}{s} + \frac{\partial S_{ss}}{\partial s} + \frac{1}{s} \frac{\partial S_{s\vartheta}}{\partial \vartheta} + \frac{\partial S_{s\zeta}}{\partial \zeta}, \\ \varrho_w \frac{\partial^2 u_{\vartheta}}{\partial t^2} &= \frac{S_{s\vartheta} + S_{\vartheta s}}{s} + \frac{\partial S_{\vartheta s}}{\partial s} + \frac{1}{s} \frac{\partial S_{\vartheta\vartheta}}{\partial \vartheta} + \frac{\partial S_{\vartheta\zeta}}{\partial \zeta}, \\ \varrho_w \frac{\partial^2 u_{\zeta}}{\partial t^2} &= \frac{S_{\zeta s}}{s} + \frac{\partial S_{\zeta s}}{\partial s} + \frac{1}{s} \frac{\partial S_{\zeta\vartheta}}{\partial \vartheta} + \frac{\partial S_{\zeta\zeta}}{\partial \zeta}, \end{aligned}$$

where ϱ_w denotes the density of the elastic solid. Equations (19) are supplemented by boundary conditions. To reflect a typical situation in blood flow modeling, we assume that the external boundary is exposed to the external ambient pressure P_e

$$\mathbf{n}_e \mathbf{S} \mathbf{n}_e = -P_e, \quad (25)$$

where \mathbf{n}_e is the outward unit normal vector on Σ_{ext} , and that the tangential displacements of the exterior boundary are zero, namely

$$u_{\vartheta}(R + h, \vartheta, \zeta, t) = 0, \quad u_{\zeta}(R + h, \vartheta, \zeta, t) = 0. \quad (26)$$

On Σ_{int}^w we impose continuity of stresses

$$\mathbf{S} \mathbf{n}_0(R, \vartheta, \zeta, t) = \mathbf{\Phi}_f \mathbf{n}_0(R, \vartheta, \zeta, t), \quad (27)$$

where \mathbf{n}_0 is the outward unit normal vector on Σ_{int}^w and $\mathbf{\Phi}_f$ is the stress due to the fluid flow in the lumen (interior) of the annulus, written in the Lagrangian framework. The fluid stress $\mathbf{\Phi}_f$ will be specified later in (41). Thus, neither the internal

or the external boundary of the structure are given explicitly. Both boundaries will be determined as a solution of the fluid-structure-ambient interaction problem.

At the end points of the annular sections we assume that the displacement is zero

$$\mathbf{u}(R, \vartheta, 0, t) = \mathbf{u}(R, \vartheta, L, t) = 0. \quad (28)$$

Although the latter set of conditions is not natural for the blood flow application, the *asymptotically reduced* problem has this set of conditions relaxed in a way that is appropriate for the use in the blood flow application. Namely, following the approach in [5] one can show that the homogeneous boundary conditions for the displacement at the inlet and at the outlet boundary are “incompatible” with the prescribed stresses at the inlet and outlet. As a consequence, a boundary layer forms near the inlet and outlet boundaries “contaminating” the solution of the full two-dimensional axially-symmetric problem in a small neighborhood. It was shown in [5] that this boundary layer decays exponentially fast away from the boundary. However, in the asymptotically reduced effective problem, studied in Section 5, conditions (28) drop out and the displacement of the structure in the reduced model will be governed entirely by the inlet and outlet fluid pressure and the conditions imposed on the external and internal boundary of the structure Σ_{ext}^w and Σ_{int}^w .

2.2. Description of the fluid. The domain occupied by the fluid is not known a priori and it will be denoted by $\Omega^f(t)$. In cylindrical coordinates (r, θ, z) the fluid domain is defined by

$$\Omega^f(t) = \{(r, \theta, z) \in \mathbf{R}^3 \mid \mathbf{r} \in (\mathbf{0}, \gamma(\theta, \mathbf{z}, t)), \theta \in [0, 2\pi), \mathbf{z} \in (\mathbf{0}, \mathbf{L})\}, \quad (29)$$

where $\gamma(\theta, z, t)$ is the fluid-solid interface given by:

$$\gamma(\theta, z, t) = R + u_s(R, \vartheta, \zeta, t), \quad (30)$$

with

$$(\theta, z, t) = (\vartheta + u_\vartheta(R, \vartheta, \zeta, t), \zeta + u_\zeta(R, \vartheta, \zeta, t), t) \quad (31)$$

relating the Eulerian coordinates of the fluid description with the Lagrangian coordinates used in the description of the structure. The inlet and outlet sections of the fluid domain are given by

$$\Sigma_0^f = \{(r, \theta, z) \in \mathbf{R}^3 \mid \mathbf{r} \in [0, \mathbf{R}), \theta \in [0, 2\pi), \mathbf{z} = \mathbf{0}\}, \quad (32)$$

$$\Sigma_L^f = \{(r, \theta, z) \in \mathbf{R}^3 \mid \mathbf{r} \in [0, \mathbf{R}), \theta \in [0, 2\pi), \mathbf{z} = \mathbf{L}\}. \quad (33)$$

The motion of the fluid is described by the Navier-Stokes equations for an incompressible, viscous fluid. In cylindrical coordinates, in the absence of body forces,

they read as follows:

$$\frac{1}{r} \frac{\partial}{\partial r}(rv_r) + \frac{1}{r} \frac{\partial v_\theta}{\partial \theta} + \frac{\partial v_z}{\partial z} = 0, \quad (34)$$

$$\varrho \left(\frac{\partial v_r}{\partial t} + v_r \frac{\partial v_r}{\partial r} + \frac{v_\theta}{r} \frac{\partial v_r}{\partial \theta} + v_z \frac{\partial v_r}{\partial z} - \frac{v_\theta^2}{r} \right) = -\frac{\partial p}{\partial r} + \mu \left(\Delta v_r - \frac{v_r}{r^2} - \frac{2}{r^2} \frac{\partial v_\theta}{\partial \theta} \right), \quad (35)$$

$$\varrho \left(\frac{\partial v_\theta}{\partial t} + v_r \frac{\partial v_\theta}{\partial r} + \frac{v_r v_\theta}{r} + \frac{v_\theta}{r} \frac{\partial v_\theta}{\partial \theta} + v_z \frac{\partial v_\theta}{\partial z} \right) = -\frac{1}{r} \frac{\partial p}{\partial \theta} + \mu \left(\Delta v_\theta - \frac{v_\theta}{r^2} + \frac{2}{r^2} \frac{\partial v_r}{\partial \theta} \right), \quad (36)$$

$$\varrho \left(\frac{\partial v_z}{\partial t} + v_r \frac{\partial v_z}{\partial r} + \frac{v_\theta}{r} \frac{\partial v_z}{\partial \theta} + v_z \frac{\partial v_z}{\partial z} \right) = -\frac{\partial p}{\partial z} + \mu \Delta v_z, \quad (37)$$

where $\mathbf{v} = (v_r, v_\theta, v_z)$ is the velocity of the fluid, p is the pressure, ϱ is the fluid density and μ is the dynamic viscosity of the fluid. We used notation Δ to denote the operator

$$\Delta \varphi = \frac{1}{r} \frac{\partial}{\partial r} \left(r \frac{\partial \varphi}{\partial r} \right) + \frac{1}{r^2} \frac{\partial^2 \varphi}{\partial \theta^2} + \frac{\partial^2 \varphi}{\partial z^2} = \Delta_r \varphi + \frac{1}{r^2} \frac{\partial^2 \varphi}{\partial \theta^2} + \frac{\partial^2 \varphi}{\partial z^2}, \quad (38)$$

applied to a scalar function $\varphi(r, \theta, z)$.

The coupling between the fluid and the structure is performed by requiring the continuity of velocity and the continuity of the stress at the interface. We write these conditions in the Lagrangian framework:

$$\mathbf{v}(\gamma(\theta, z, t), \theta, z, t) = \frac{\partial \mathbf{u}}{\partial t}(R, \vartheta, \zeta, t) \quad (39)$$

with (θ, z, t) defined in (31), while the condition on the stress reads

$$\det(\mathbf{F}) \boldsymbol{\sigma} \mathbf{F}^{-t} \mathbf{n}_0 = \mathbf{S} \mathbf{n}_0, \quad (40)$$

where $\mathbf{n}_0 = (-1, 0, 0)$ is the outer unit normal on Σ_0^w . Here

$$\det(\mathbf{F}) \boldsymbol{\sigma} \mathbf{F}^{-t} =: \boldsymbol{\Phi}_f \quad (41)$$

is the Lagrangian form of the fluid stress $\boldsymbol{\sigma} = -p\mathbf{I} + 2\mu\mathbf{D}(\mathbf{v})$, $\mathbf{F} = \mathbf{I} + \nabla \mathbf{u}$ is the gradient of the transformation between the Eulerian and Lagrangian coordinates, and $\mathbf{D}(\mathbf{v}) = (\nabla \mathbf{v} + (\nabla \mathbf{v})^t)/2$ is the symmetrized gradient of the fluid velocity, given, in cylindrical coordinates, by the following

$$\mathbf{D}(\mathbf{v}) = \begin{pmatrix} \frac{\partial v_r}{\partial r} & \frac{1}{2} \left(\frac{1}{r} \frac{\partial v_r}{\partial \theta} + \frac{\partial v_\theta}{\partial r} - \frac{v_\theta}{r} \right) & \frac{1}{2} \left(\frac{\partial v_r}{\partial z} + \frac{\partial v_z}{\partial r} \right) \\ \frac{1}{2} \left(\frac{1}{r} \frac{\partial v_r}{\partial \theta} + \frac{\partial v_\theta}{\partial r} - \frac{v_\theta}{r} \right) & \frac{1}{r} \frac{\partial v_\theta}{\partial \theta} + \frac{v_r}{r} & \frac{1}{2} \left(\frac{1}{r} \frac{\partial v_z}{\partial \theta} + \frac{\partial v_\theta}{\partial z} \right) \\ \frac{1}{2} \left(\frac{\partial v_r}{\partial z} + \frac{\partial v_z}{\partial r} \right) & \frac{1}{2} \left(\frac{1}{r} \frac{\partial v_z}{\partial \theta} + \frac{\partial v_\theta}{\partial z} \right) & \frac{\partial v_z}{\partial z} \end{pmatrix}.$$

At the inlet and outlet boundary we require that the pressure be prescribed and the flow enters and leaves the domain parallel to the axis of symmetry. This gives

$$v_r = 0 \quad \text{and} \quad p = P_{0/L}(t) \quad \text{at} \quad z = 0, L. \quad (42)$$

Remark. In the follow-up paper [2] we show that the kinematic lateral boundary condition (39) determines a new time-scale necessary for the asymptotic analysis

of the coupling between the non-stationary Navier-Stokes problem and the three-dimensional elastic structure. This new time-scale interpolates between the time scale at which the oscillations in the structure take place (fast traveling waves) and the time scale determined by the velocity of the fluid. It is only with this new time scale that a closed system of equations can be obtained. Nothing like this is necessary in the stationary Stokes case, as we shall see in the next section. Thus, the two cases differ not only in the traditional sense, but also in the choice of the time scale necessary for a derivation of a closed set of reduced equations.

3. The Stationary, Axially Symmetric Stokes Fluid-Structure Interaction Problem: Summary. In this manuscript we focus on the fluid-structure interaction problem assuming axially symmetric, stationary Stokes flow. The axial symmetry means, in particular, that the following holds

Assumption 1. All the quantities are independent of the azimuthal variables θ and ϑ and the azimuthal components of the displacement and of the fluid velocity are both equal to zero $v_\theta = u_\vartheta = 0$.

The stationary feature of the problem implies that the fluid velocity, the pressure and the structure displacement are all independent of time.

Under these assumptions the flow equations simplify to

$$\frac{1}{r} \frac{\partial}{\partial r} (r v_r) + \frac{\partial v_z}{\partial z} = 0, \quad (43)$$

$$-\frac{\partial p}{\partial r} + \mu \left(\Delta_r v_r + \frac{\partial^2 v_r}{\partial z^2} - \frac{v_r}{r^2} \right) = 0, \quad (44)$$

$$-\frac{\partial p}{\partial z} + \mu \left(\Delta_r v_z + \frac{\partial^2 v_z}{\partial z^2} \right) = 0, \quad (45)$$

where $\Delta_r := \frac{1}{r} \frac{\partial}{\partial r} \left(r \frac{\partial}{\partial r} \right)$. These equations are defined on the domain

$$\Omega^f = \{(r \cos \theta, r \sin \theta, z) | 0 < r < \gamma(z), z \in (0, L), \theta \in (0, 2\pi)\} \quad (46)$$

bounded by the fluid-structure interface

$$\gamma(z) = R + u_s(R, \zeta), \quad (47)$$

where $z = \zeta + u_\zeta(R, \zeta)$. Here u_s and u_ζ are the radial and axial displacement of the structure, evaluated at $s = R$. The fluid equations are defined in the Eulerian coordinates where r denotes the radial, and z the axial variable, while the structure is defined in the Lagrangian coordinates where s denotes the radial, and ζ the axial variable.

The structure equilibrium equations, determining the displacement (u_s, u_ζ) read

$$\frac{S_{ss} - S_{\vartheta\vartheta}}{s} + \frac{\partial S_{ss}}{\partial s} + \frac{\partial S_{s\zeta}}{\partial \zeta} = 0, \quad (48)$$

$$\frac{S_{\zeta s}}{s} + \frac{\partial S_{\zeta s}}{\partial s} + \frac{\partial S_{\zeta\zeta}}{\partial \zeta} = 0, \quad (49)$$

where

$$\mathbf{S} = \mathbf{L} + \mathbf{Q} \quad (50)$$

with

$$\mathbf{L} = \begin{bmatrix} 2\mu_w \frac{\partial u_s}{\partial s} + \lambda_w \operatorname{div} \mathbf{u} & 0 & 2\mu_w e_{s\zeta} \\ 0 & 2\mu_w \frac{u_s}{s} + \lambda_w \operatorname{div} \mathbf{u} & 0 \\ 2\mu_w e_{s\zeta} & 0 & 2\mu_w \frac{\partial u_\zeta}{\partial \zeta} + \lambda_w \operatorname{div} \mathbf{u} \end{bmatrix} \quad (51)$$

and

$$\mathbf{Q} = \begin{bmatrix} T_{ss} & 0 & w_{s\zeta} T_{\zeta\zeta} + \frac{1}{2} e_{s\zeta} (T_{\zeta\zeta} - T_{ss}) \\ 0 & T_{\theta\theta} & 0 \\ -w_{s\zeta} T_{ss} - \frac{1}{2} e_{s\zeta} (T_{\zeta\zeta} - T_{ss}) & 0 & T_{\zeta\zeta} \end{bmatrix}, \quad (52)$$

where

$$w_{s\zeta} = \frac{1}{2} \left(\frac{\partial u_s}{\partial \zeta} - \frac{\partial u_\zeta}{\partial s} \right), \quad e_{s\zeta} = \frac{1}{2} \left(\frac{\partial u_s}{\partial \zeta} + \frac{\partial u_\zeta}{\partial s} \right). \quad (53)$$

The boundary conditions for the structure at $\zeta = 0$ and $\zeta = L$ are given by:

$$\mathbf{u}(s, 0) = \mathbf{u}(s, L) = 0, \quad s \in (R, R + h). \quad (54)$$

At the external cylindrical boundary the structure is exposed to the ambient pressure P_e and the axial displacement is equal to zero:

$$\mathbf{n}_e \mathbf{S} \mathbf{n}_e|_{\Sigma_{\text{ext}}} = -P_e, \quad u_\zeta(R + h, \zeta) = 0, \quad (55)$$

where $\mathbf{n}_e = (1, 0, 0)$. At the internal cylindrical boundary Σ_0^w the structure is coupled with the fluid through the stationary form of the kinematic and dynamic boundary condition, respectively:

$$\mathbf{v}(\gamma(z), z) = (0, 0), \quad \det(\mathbf{F}) \boldsymbol{\sigma} \mathbf{F}^{-t} \mathbf{n}_0|_{\Sigma_{\text{int}}} = \mathbf{S} \mathbf{n}_0, \quad (56)$$

where $\mathbf{n}_0 = (-1, 0, 0)$ is the outer unit normal on Σ_0^w , and $\mathbf{F} = \mathbf{I} + \nabla \mathbf{u}$ is the gradient of the transformation between the Eulerian and Lagrangian coordinates, with $\boldsymbol{\sigma} = -p \mathbf{I} + 2\mu \mathbf{D}(\mathbf{v})$ denoting the fluid stress. Finally, at the inlet and outlet boundary of the fluid domain Ω^f , we require that the pressure be prescribed and that the flow enters and leaves the domain parallel to the axis of symmetry:

$$v_r = 0 \quad \text{and} \quad p = P_{0/L} \quad \text{at} \quad z = 0, L. \quad (57)$$

4. The non-dimensional variables. To introduce the scalings of the independent variables, recall that we consider a three-dimensional elastic cylinder in the case when the radius R of the lumen is comparable to the thickness h of the elastic cylinder, namely $h = O(R)$. Thus, the radial variables for the fluid and the structure are scaled with the same parameter as

$$r = R\tilde{r}, \quad s = R\tilde{s}, \quad (58)$$

so that $\tilde{s} \in (1, 1 + h/R)$ for the elastic cylinder. In particular, we are interested in the reduced, effective model when the aspect ratio

$$\epsilon = \frac{R}{L} = \frac{h}{L}$$

is small. The cylinder length L gives the scaling for the axial variables

$$z = L\tilde{z}, \quad \zeta = L\tilde{\zeta}. \quad (59)$$

The dependent variables are scaled as follows: the two components of the displacement

$$u_s(s, \zeta) = U_s \tilde{u}_s(\tilde{s}, \tilde{\zeta}), \quad u_\zeta(s, \zeta) = U_\zeta \tilde{u}_\zeta(\tilde{s}, \tilde{\zeta}) \quad (60)$$

and the fluid velocity and pressure are scaled as

$$v_r(r, z) = V_r \tilde{v}_r(\tilde{r}, \tilde{z}), \quad v_z(r, z) = V_z \tilde{v}_z(\tilde{r}, \tilde{z}), \quad p(r, z) = P \tilde{p}(\tilde{r}, \tilde{z}). \quad (61)$$

Finally we introduce the characteristic scale for the residual stress tensor to be τ so that

$$\mathbf{T} = \tau \tilde{\mathbf{T}}. \quad (62)$$

The pre-stress scale τ is around 10^3 Pa, as shown in Section 2.1.1, Figure 5.

With these scalings, the non-dimensional reference domain for the elastic structure becomes

$$\tilde{\Omega}_0^w = \{(\tilde{s} \cos \vartheta, \tilde{s} \sin \vartheta, \tilde{\zeta}) \in \mathbf{R}^3 \mid \tilde{\mathbf{s}} \in (\mathbf{1}, \mathbf{1} + \mathbf{h}/\mathbf{R}), \vartheta \in [0, 2\pi), \tilde{\zeta} \in (0, \mathbf{1})\}, \quad (63)$$

while the fluid domain in non-dimensional variables is given by

$$\tilde{\Omega}^f = \{(\tilde{r} \cos \theta, \tilde{r} \sin \theta, \tilde{z}) \in \mathbf{R}^3 \mid \tilde{\mathbf{r}} \in (\mathbf{0}, \tilde{\gamma}(\tilde{\mathbf{z}})), \theta \in [0, 2\pi), \tilde{\mathbf{z}} \in (0, \mathbf{1})\}, \quad (64)$$

where $\tilde{\gamma}(\tilde{z}) = \gamma(z)/R$.

4.1. The Fluid Equations. By plugging the non-dimensional variables into the fluid equations (43)-(45), we obtain the following system of fluid equations in non-dimensional form. The incompressibility condition becomes:

$$\frac{V_r}{V_z} \frac{L}{R} \frac{1}{\tilde{r}} \frac{\partial}{\partial \tilde{r}}(\tilde{r} \tilde{v}_r) + \frac{\partial \tilde{v}_z}{\partial \tilde{z}} = 0, \quad (65)$$

and the momentum equations read

$$-\frac{PR}{\mu V_r} \frac{\partial \tilde{p}}{\partial \tilde{r}} + \Delta_{\tilde{r}} \tilde{v}_r - \frac{\tilde{v}_r}{\tilde{r}^2} + \epsilon^2 \frac{\partial^2 \tilde{v}_r}{\partial \tilde{z}^2} = 0 \quad (66)$$

$$-\frac{PR^2}{\mu L V_z} \frac{\partial \tilde{p}}{\partial \tilde{z}} + \Delta_{\tilde{r}} \tilde{v}_z + \epsilon^2 \frac{\partial^2 \tilde{v}_z}{\partial \tilde{z}^2} = 0, \quad (67)$$

where we recall that $\epsilon = R/L$. From the incompressibility condition it follows that a consistent scaling for the velocity components is given by $V_r = \epsilon V_z$, [7]. To determine the appropriate scaling for the pressure we follow the approach based on the homogenization theory for porous media flows, presented in [7]. Determining the ‘‘correct’’ scaling for the pressure is important for several reasons, one of which is that the correct scaling for the pressure will give rise to a reduced system that is closed. Following [7] we obtain $P = \mu V_z / (L \epsilon^2)$, which is of ‘‘Poiseuille type’’. With these choices the Stokes equations become

$$\frac{1}{\tilde{r}} \frac{\partial}{\partial \tilde{r}}(\tilde{r} \tilde{v}_r) + \frac{\partial \tilde{v}_z}{\partial \tilde{z}} = 0, \quad (68)$$

$$-\frac{1}{\epsilon^2} \frac{\partial \tilde{p}}{\partial \tilde{r}} + \Delta_{\tilde{r}} \tilde{v}_r - \frac{\tilde{v}_r}{\tilde{r}^2} + \epsilon^2 \frac{\partial^2 \tilde{v}_r}{\partial \tilde{z}^2} = 0 \quad (69)$$

$$-\frac{\partial \tilde{p}}{\partial \tilde{z}} + \Delta_{\tilde{r}} \tilde{v}_z + \epsilon^2 \frac{\partial^2 \tilde{v}_z}{\partial \tilde{z}^2} = 0. \quad (70)$$

In particular, the following is the non-dimensional form of the fluid stress tensor $\tilde{\sigma}$:

$$\boldsymbol{\sigma} = \frac{\mu V_z}{\epsilon^2 L} \tilde{\boldsymbol{\sigma}} = \frac{\mu V_z}{\epsilon^2 L} \begin{bmatrix} -\tilde{p} + 2\epsilon^2 \frac{\partial \tilde{v}_r}{\partial \tilde{r}} & 0 & \epsilon^3 \frac{\partial \tilde{v}_r}{\partial \tilde{z}} + \epsilon \frac{\partial \tilde{v}_z}{\partial \tilde{r}} \\ 0 & -\tilde{p} + 2\epsilon^2 \frac{\tilde{v}_r}{\tilde{r}} & 0 \\ \epsilon^3 \frac{\partial \tilde{v}_r}{\partial \tilde{z}} + \epsilon \frac{\partial \tilde{v}_z}{\partial \tilde{r}} & 0 & -\tilde{p} + 2\epsilon^2 \frac{\partial \tilde{v}_z}{\partial \tilde{z}} \end{bmatrix}. \quad (71)$$

To obtain the effective equations that approximate the original, three-dimensional axially symmetric problem to ϵ^2 accuracy, we expand the dependent variables with

respect to ϵ , plug the expansions into the non-dimensional equations, and ignore the terms of order ϵ^2 and smaller. The expansion of the dependent variables is given by the following:

$$\begin{pmatrix} v_z \\ v_r \end{pmatrix} = \begin{pmatrix} V_z \tilde{v}_z \\ V_r \tilde{v}_r \end{pmatrix} = \begin{pmatrix} V_z (\tilde{v}_z^0 + \epsilon \tilde{v}_z^1 + \dots) \\ V_z \epsilon (\tilde{v}_r^1 + \dots) \end{pmatrix}, p = \frac{\mu V_z}{\epsilon^2 L} \tilde{p} = \frac{\mu V_z}{\epsilon^2 L} (\tilde{p}^0 + \epsilon \tilde{p}^1 + \dots). \quad (72)$$

Then, the divergence free condition up to $O(\epsilon^2)$ reads:

$$\frac{1}{\tilde{r}} \frac{\partial}{\partial \tilde{r}} (\tilde{r} \tilde{v}_r^1) + \frac{\partial \tilde{v}_z^0}{\partial \tilde{z}} = 0. \quad (73)$$

The balance of radial momentum implies that the pressure is hydrostatic up to the second order:

$$\tilde{p}^0 = \tilde{p}^0(\tilde{z}), \quad \tilde{p}^1 = \tilde{p}^1(\tilde{z}), \quad (74)$$

and the balance of axial momentum at ϵ^0 and ϵ implies, respectively:

$$2 \frac{\partial \tilde{v}_z^0}{\partial \tilde{r}} = \tilde{r} \frac{d\tilde{p}^0}{d\tilde{z}} \quad \text{and} \quad 2 \frac{\partial \tilde{v}_z^1}{\partial \tilde{r}} = \tilde{r} \frac{d\tilde{p}^1}{d\tilde{z}}. \quad (75)$$

4.2. The Structure Equations. To study the leading-order problem for the structure we will be assuming the following

Assumption 2. The radial and the axial displacement of the structure are of the same order of magnitude, namely

$$U_s = U_\zeta = \delta, \quad (76)$$

where $\delta < h$.

Under this assumption the non-dimensional form of the incremental elasticity tensor L becomes

$$\mathbf{L} = \mu_w \tilde{\mathbf{L}} = \mu_w \frac{\delta}{R} \begin{bmatrix} 2 \frac{\partial \tilde{u}_s}{\partial \tilde{s}} + \frac{\lambda_w}{\mu_w} \widetilde{div} \tilde{\mathbf{u}} & 0 & \epsilon \frac{\partial \tilde{u}_s}{\partial \tilde{\zeta}} + \frac{\partial \tilde{u}_\zeta}{\partial \tilde{s}} \\ 0 & 2 \frac{\tilde{u}_s}{\tilde{s}} + \frac{\lambda_w}{\mu_w} \widetilde{div} \tilde{\mathbf{u}} & 0 \\ \epsilon \frac{\partial \tilde{u}_s}{\partial \tilde{\zeta}} + \frac{\partial \tilde{u}_\zeta}{\partial \tilde{s}} & 0 & 2\epsilon \frac{\partial \tilde{u}_\zeta}{\partial \tilde{\zeta}} + \frac{\lambda_w}{\mu_w} \widetilde{div} \tilde{\mathbf{u}} \end{bmatrix}, \quad (77)$$

where

$$\widetilde{div} \tilde{\mathbf{u}} = \left(\frac{1}{\tilde{s}} \frac{\partial}{\partial \tilde{s}} (\tilde{s} \tilde{u}_s) + \epsilon \frac{\partial \tilde{u}_\zeta}{\partial \tilde{\zeta}} \right). \quad (78)$$

Similarly, the contribution from residual stress Q in non-dimensional variables reads

$$\mathbf{Q} = \tau \tilde{\mathbf{Q}} = \tau \begin{bmatrix} \tilde{T}_{ss} & 0 & \tilde{w}_{s\zeta} \tilde{T}_{\zeta\zeta} + \frac{1}{2} \tilde{e}_{s\zeta} (\tilde{T}_{\zeta\zeta} - \tilde{T}_{ss}) \\ 0 & \tilde{T}_{\theta\theta} & 0 \\ -\tilde{w}_{s\zeta} \tilde{T}_{ss} - \frac{1}{2} \tilde{e}_{s\zeta} (\tilde{T}_{\zeta\zeta} - \tilde{T}_{ss}) & 0 & \tilde{T}_{\zeta\zeta} \end{bmatrix}, \quad (79)$$

where

$$\tilde{w}_{s\zeta} = \frac{1}{2} \frac{\delta}{R} \left(\epsilon \frac{\partial \tilde{u}_s}{\partial \tilde{\zeta}} - \frac{\partial \tilde{u}_\zeta}{\partial \tilde{s}} \right), \quad \tilde{e}_{s\zeta} = \frac{1}{2} \frac{\delta}{R} \left(\epsilon \frac{\partial \tilde{u}_s}{\partial \tilde{\zeta}} + \frac{\partial \tilde{u}_\zeta}{\partial \tilde{s}} \right). \quad (80)$$

The radial and axial component of the non-dimensional equilibrium equations (19) describing the structure equilibrium for the stationary problem are then given by:

$$0 = \frac{\tilde{S}_{ss} - \tilde{S}_{\vartheta\vartheta}}{\tilde{s}} + \frac{\partial \tilde{S}_{ss}}{\partial \tilde{s}} + \epsilon \frac{\partial \tilde{S}_{s\zeta}}{\partial \tilde{\zeta}}, \quad (81)$$

$$0 = \frac{1}{\tilde{s}} \frac{\partial}{\partial \tilde{s}} (\tilde{s} \tilde{S}_{\zeta s}) + \epsilon \frac{\partial \tilde{S}_{\zeta\zeta}}{\partial \tilde{\zeta}}, \quad (82)$$

where $\tilde{\mathbf{S}} = \tilde{\mathbf{L}} + \frac{\tau}{\mu_w} \tilde{\mathbf{Q}}$ so that $\mathbf{S} = \mu_w \tilde{\mathbf{S}}$. In the rest of the manuscript we will be using the following assumption:

Assumption 3. The scaling μ_w for the incremental elasticity tensor L is of the same order of magnitude or bigger than the scaling τ for the residual stress T .

We will see that this assumption is reasonable for the blood flow application. In fact, as shown in Section 2.1.1, for the data presented in [9, 11] τ is around 10^3 Pa, whereas μ_w , for the blood flow application, is around 10^5 Pa. Thus, τ is smaller than μ_w , which is in agreement with our analysis.

By expanding the structure dependent variables with respect to ϵ :

$$\tilde{u}_s = \tilde{u}_s^0 + \epsilon \tilde{u}_s^1 + O(\epsilon^2), \quad \tilde{u}_\zeta = \tilde{u}_\zeta^0 + \epsilon \tilde{u}_\zeta^1 + O(\epsilon^2), \quad (83)$$

and plugging the expansions into equations (81), (82), we get the following leading order equilibrium equations for the structure displacement $\mathbf{u}^0 = (\tilde{u}_s^0, \tilde{u}_\zeta^0)$

$$\left(2 + \frac{\lambda_w}{\mu_w}\right) \frac{\partial}{\partial \tilde{s}} \left[\frac{1}{\tilde{s}} \frac{\partial}{\partial \tilde{s}} (\tilde{s} \tilde{u}_s^0) \right] = -\frac{\tau}{\mu_w} \frac{R}{\delta} \left(\frac{\tilde{T}_{ss} - \tilde{T}_{\vartheta\vartheta}}{\tilde{s}} + \frac{\partial \tilde{T}_{ss}}{\partial \tilde{s}} \right), \quad (84)$$

$$\left(2 + \frac{3\tau}{4\mu_w} \tilde{T}_{ss} - \frac{\tau}{4\mu_w} \tilde{T}_{\zeta\zeta}\right) \frac{\partial \tilde{u}_\zeta^0}{\partial \tilde{s}} = \frac{C_0(\tilde{\zeta})}{\tilde{s}}, \quad (85)$$

defined for $(\tilde{s}, \tilde{\zeta}) \in (1, 1 + h/R) \times (0, 1)$. Notice that the equation of the equilibrium for the stress tensor \mathbf{T} , (15), implies that the right hand-side of (84) is zero. Thus, the zero-th order displacement $\mathbf{u}^0 = (\tilde{u}_s^0, \tilde{u}_\zeta^0)$ satisfies

$$\frac{\partial}{\partial \tilde{s}} \left[\frac{1}{\tilde{s}} \frac{\partial}{\partial \tilde{s}} (\tilde{s} \tilde{u}_s^0) \right] = 0, \quad (86)$$

$$\left(1 + \frac{3\tau}{4\mu_w} \tilde{T}_{ss} - \frac{\tau}{4\mu_w} \tilde{T}_{\zeta\zeta}\right) \frac{\partial \tilde{u}_\zeta^0}{\partial \tilde{s}} = \frac{C_0(\tilde{\zeta})}{\tilde{s}}. \quad (87)$$

Similarly, a calculation shows that the ϵ -correction $(\tilde{u}_s^1, \tilde{u}_\zeta^1)$ of the displacement $\mathbf{u} = \mathbf{u}^0 + \epsilon \mathbf{u}^1$ satisfies the following equations in the radial and axial direction respectively

$$\left(2 + \frac{\lambda_w}{\mu_w}\right) \frac{\partial}{\partial \tilde{s}} \left[\frac{1}{\tilde{s}} \frac{\partial}{\partial \tilde{s}} (\tilde{s} \tilde{u}_s^1) \right] = - \left[\left(1 + \frac{\lambda_w}{\mu_w}\right) - \frac{\tau}{4\mu_w} (\tilde{T}_{\zeta\zeta} + \tilde{T}_{ss}) \right] \frac{\partial^2 \tilde{u}_s^0}{\partial \tilde{\zeta} \partial \tilde{s}}, \quad (88)$$

$$\left(1 + \frac{3\tau}{4\mu_w} \tilde{T}_{ss} - \frac{\tau}{4\mu_w} \tilde{T}_{\zeta\zeta}\right) \frac{\partial \tilde{u}_\zeta^1}{\partial \tilde{s}} = \frac{C_1(\tilde{\zeta})}{\tilde{s}} - \left[\left(1 + \frac{\lambda_w}{\mu_w}\right) - \frac{\tau}{4\mu_w} (\tilde{T}_{\zeta\zeta} + \tilde{T}_{ss}) \right] \frac{\partial \tilde{u}_s^0}{\partial \tilde{\zeta}}. \quad (89)$$

The expansion of the interface γ , defined in (30), is determined by both the radial and axial displacement. The expansion for the radial displacement enters explicitly, whereas the expansion of the axial displacement enters through the relationship between the Eulerian and Lagrangian coordinates as follows:

$$\gamma(z) = R + u_s(R, \zeta) = R \left[1 + \frac{\delta}{R} \left(\tilde{u}_s^0(1, \tilde{\zeta}) + \epsilon \tilde{u}_s^1(1, \tilde{\zeta}) \right) \right] = R [\tilde{\gamma}^0 + \epsilon \tilde{\gamma}^1], \quad (90)$$

with

$$\tilde{\gamma}^0(\tilde{z}) := 1 + \frac{\delta}{R} \tilde{u}_s^0(1, \tilde{\zeta}) \quad \text{and} \quad \tilde{\gamma}^1(\tilde{z}) := \frac{\delta}{R} \tilde{u}_s^1(1, \tilde{\zeta}), \quad (91)$$

where $z = \zeta + u_\zeta(R, \zeta)$ implies

$$\tilde{z} = \tilde{\zeta} + \frac{\delta}{L} \tilde{u}_\zeta(1, \tilde{\zeta}) = \tilde{\zeta} + \epsilon \frac{\delta}{R} \tilde{u}_\zeta(1, \tilde{\zeta}) = \tilde{\zeta} + \epsilon \frac{\delta}{R} \tilde{u}_\zeta^0 + O(\epsilon^2). \quad (92)$$

As we shall see later, for the physiologically relevant external boundary conditions given by (26), the longitudinal displacement u_ζ^0 will turn out to be zero throughout the structure, implying

$$\tilde{z} = \tilde{\zeta} + O(\epsilon^2). \quad (93)$$

This will imply that only the radial displacement determines the position of the fluid-solid interface up to the $O(\epsilon^2)$ -order.

4.3. The Fluid-Structure Coupling. To couple the structure and the fluid equations, integrate the balance of axial momentum (70) with respect to \tilde{r} from \tilde{r} to $\tilde{\gamma}(\tilde{z})$ and use the no-slip boundary condition in (56). After collecting the terms of order ϵ^0 and ϵ^1 one obtains the following expressions for \tilde{v}_z^0 and \tilde{v}_z^1 respectively:

$$\tilde{v}_z^0(\tilde{r}, \tilde{z}) = \frac{1}{4} [\tilde{r}^2 - (\tilde{\gamma}^0(\tilde{z}))^2] \frac{d\tilde{p}^0}{d\tilde{z}}(\tilde{z}), \quad (94)$$

$$\tilde{v}_z^1(\tilde{r}, \tilde{z}) = \frac{1}{4} [\tilde{r}^2 - (\tilde{\gamma}^0(\tilde{z}))^2] \frac{d\tilde{p}^1}{d\tilde{z}}(\tilde{z}) - \frac{1}{2} \tilde{\gamma}^0 \tilde{\gamma}^1 \frac{\partial \tilde{p}^0}{\partial \tilde{z}}. \quad (95)$$

These equations define the axial component of the velocity in terms of the pressure \tilde{p} and the interface $\tilde{\gamma}$.

Next we obtain the expressions for the radial component of the velocity in terms of \tilde{p} and $\tilde{\gamma}$ by plugging the expressions for the axial component of the velocity (94) and (95) into the incompressibility condition (73), and by integrating with respect to \tilde{r} from 0 to \tilde{r} . The equation at the ϵ^1 order gives

$$\tilde{v}_r^1(\tilde{r}, \tilde{z}) = \frac{\tilde{r}}{4} \tilde{\gamma}^0 \frac{d\tilde{\gamma}^0}{d\tilde{z}} \frac{d\tilde{p}^0}{d\tilde{z}} - \frac{\tilde{r}^3}{16} \frac{d^2\tilde{p}^0}{d\tilde{z}^2} + \frac{\tilde{r}}{8} (\tilde{\gamma}^0)^2 \frac{d^2\tilde{p}^0}{d\tilde{z}^2}. \quad (96)$$

At this point we have expressed the axial and the radial component of the velocity in terms of the pressure \tilde{p} and the fluid-structure interface $\tilde{\gamma}$. We now derive an equation that relates the pressure and the interface. This will lead to a result which is a generalization of the well-known fact that the pressure gradient is constant for the Poiseuille flow in the stationary Stokes problem through an axially symmetric domain with fixed walls. With deformable walls, we will see that the effective pressure gradient is not constant, but inversely proportional to the fourth power of the structure displacement at the interface. More precisely, by integrating the incompressibility condition with respect to \tilde{r} from 0 to $\tilde{\gamma}$ we get

$$\int_0^{\tilde{\gamma}(\tilde{z})} \frac{\partial}{\partial \tilde{r}} (\tilde{r} \tilde{v}_r) d\tilde{r} + \int_0^{\tilde{\gamma}(\tilde{z})} \frac{\partial \tilde{v}_z}{\partial \tilde{z}} \tilde{r} d\tilde{r} = 0, \quad (97)$$

and then recalling the no-slip condition $\tilde{v}_r(\tilde{\gamma}(\tilde{z}), \tilde{z}) = \tilde{v}_z(\tilde{\gamma}(\tilde{z}), \tilde{z}) = 0$ we get that the average over the cross-section of the axial component of the velocity is constant, to all orders, in \tilde{z} :

$$\frac{\partial}{\partial \tilde{z}} \int_0^{\tilde{\gamma}(\tilde{z})} \tilde{v}_z \tilde{r} d\tilde{r} = 0. \quad (98)$$

By expanding $\tilde{\gamma}$ and \tilde{v}_z and by using the expressions for \tilde{v}_z^0 and \tilde{v}_z^1 , given by (94) and (95), equation (98) implies the following pressure-interface laws at the ϵ^0 and ϵ order, respectively:

$$\frac{d}{d\tilde{z}} \left[(\tilde{\gamma}^0(\tilde{z}))^4 \frac{d\tilde{p}^0}{d\tilde{z}}(\tilde{z}) \right] = 0, \quad (99)$$

$$\frac{d}{d\tilde{z}} \left[(\tilde{\gamma}^0(\tilde{z}))^4 \frac{d\tilde{p}^1}{d\tilde{z}}(\tilde{z}) \right] = -4 \left((\tilde{\gamma}^0)^4 \frac{d\tilde{p}^0}{d\tilde{z}} \right) \frac{d}{d\tilde{z}} \left(\frac{\tilde{\gamma}^1}{\tilde{\gamma}^0} \right). \quad (100)$$

At this point, the velocity ($\tilde{v}_z^0 + \epsilon \tilde{v}_z^1, \epsilon \tilde{v}_r^1$) and the pressure $\tilde{p}^0 + \epsilon \tilde{p}^1$ can all be expressed in terms of the two functions $\tilde{\gamma}^0$ and $\tilde{\gamma}^1$ determining the fluid-structure interface $\tilde{\gamma}^0 + \epsilon \tilde{\gamma}^1$. To obtain a closed system we need equations that determine $\tilde{\gamma}^0$ and $\tilde{\gamma}^1$, or, from (91), \tilde{u}_s^0 and \tilde{u}_s^1 at $\tilde{s} = 1$. They will be provided by employing the interface condition (40) describing continuity of stresses at the fluid-solid interface. More precisely, from the fluid side we need to compute $\det(\mathbf{F})\boldsymbol{\sigma}\mathbf{F}^{-t}\mathbf{n}_0$ at $\tilde{s} = 1$ and set it equal to $\mathbf{S}\mathbf{n}_0$. For this purpose denote $\mathbf{e}_s = (1, 0, 0)$ and $\mathbf{e}_\zeta = (0, 0, 1)$. Recalling that $\tilde{T}_{ss}|_{\tilde{s}=1} = 0$, and that $\mathbf{n}_0 = -\mathbf{e}_s$, the condition $\det(\mathbf{F})\boldsymbol{\sigma}\mathbf{F}^{-t}\mathbf{n}_0 = \mathbf{S}\mathbf{n}_0$ at the ϵ^0 -order gives

$$\begin{aligned} \left(1 + \frac{\delta}{R} \frac{\tilde{u}_s^0}{\tilde{s}} \Big|_{\tilde{s}=1} \right) \tilde{p}^0 \mathbf{e}_s &= - \frac{\delta \mu_w}{PR} \left[\left(2 + \frac{\lambda_w}{\mu_w} \right) \frac{\partial \tilde{u}_s^0}{\partial \tilde{s}} \Big|_{\tilde{s}=1} + \frac{\lambda_w}{\mu_w} \frac{\tilde{u}_s^0}{\tilde{s}} \Big|_{\tilde{s}=1} \right] \mathbf{e}_s \\ &\quad - \frac{\delta \mu_w}{PR} \left[1 - \frac{\tau}{4\mu_w} \tilde{T}_{\zeta\zeta} \Big|_{\tilde{s}=1} \right] \frac{\partial \tilde{u}_\zeta^0}{\partial \tilde{s}} \Big|_{\tilde{s}=1} \mathbf{e}_\zeta. \end{aligned} \quad (101)$$

This says that in the radial direction \mathbf{e}_s we have

$$\left(1 + \frac{\delta}{R} \frac{\tilde{u}_s^0}{\tilde{s}} \Big|_{\tilde{s}=1} \right) \tilde{p}^0 = - \frac{\delta \mu_w}{PR} \left[\left(2 + \frac{\lambda_w}{\mu_w} \right) \frac{\partial \tilde{u}_s^0}{\partial \tilde{s}} \Big|_{\tilde{s}=1} + \frac{\lambda_w}{\mu_w} \frac{\tilde{u}_s^0}{\tilde{s}} \Big|_{\tilde{s}=1} \right], \quad (102)$$

and in the axial direction \mathbf{e}_ζ we obtain that there is no effective elastic shear at the interface:

$$\frac{\partial \tilde{u}_\zeta^0}{\partial \tilde{s}}(1, \tilde{\zeta}) = 0. \quad (103)$$

A similar calculation gives the ϵ -correction of the interface condition $\det(\mathbf{F})\boldsymbol{\sigma}\mathbf{F}^{-t}\mathbf{n}_0 = \mathbf{S}\mathbf{n}_0$. More precisely, in the radial direction \mathbf{e}_s we have:

$$\begin{aligned} &\left(1 + \frac{\delta}{R} \frac{\tilde{u}_s^0}{\tilde{s}} \Big|_{\tilde{s}=1} \right) \left(\tilde{p}^1 + \frac{\delta}{R} \frac{\partial \tilde{u}_\zeta^0}{\partial \tilde{\zeta}} \Big|_{\tilde{s}=1} \tilde{p}^0 \right) + \frac{\delta}{R} \frac{\tilde{u}_s^1}{\tilde{s}} \Big|_{\tilde{s}=1} \tilde{p}^0 \\ &= - \frac{\delta \mu_w}{PR} \left[\left(2 + \frac{\lambda_w}{\mu_w} \right) \frac{\partial \tilde{u}_s^1}{\partial \tilde{s}} \Big|_{\tilde{s}=1} + \frac{\lambda_w}{\mu_w} \frac{\tilde{u}_s^1}{\tilde{s}} \Big|_{\tilde{s}=1} \right] \end{aligned} \quad (104)$$

and in the axial direction \mathbf{e}_ζ :

$$\begin{aligned} &\left\{ \frac{\partial \tilde{v}_z^0}{\partial \tilde{r}} \Big|_{\tilde{s}=1} + \frac{\delta}{R} \tilde{p}^0 \frac{\partial \tilde{u}_s^0}{\partial \tilde{\zeta}} \Big|_{\tilde{s}=1} \right\} \left(1 + \frac{\delta}{R} \frac{\tilde{u}_s^0}{\tilde{s}} \Big|_{\tilde{s}=1} \right) \\ &= \frac{\delta \mu_w}{PR} \left(1 - \frac{\tau}{4\mu_w} T_{\zeta\zeta} \Big|_{\tilde{s}=1} \right) \left(\frac{\partial \tilde{u}_s^0}{\partial \tilde{\zeta}} \Big|_{\tilde{s}=1} + \frac{\partial \tilde{u}_\zeta^1}{\partial \tilde{s}} \Big|_{\tilde{s}=1} \right). \end{aligned} \quad (105)$$

These condition will now be used to determine the leading-order solution and the ϵ -correction of the fluid-structure interaction problem for the stationary Stokes problem.

5. The 0th-order solution. First notice that equation (103) says that the radial derivative of the leading-order approximation of the axial displacement is zero at the fluid-structure interface as a consequence of the fact that the axial component of the fluid stress exerted to the structure interface is negligible. This implies that the function $C_0(\tilde{\zeta})$ in (85) must equal zero, and so $\partial\tilde{u}_\zeta^0/\partial\tilde{s} = 0$ identically. Therefore, the axial component of the displacement, \tilde{u}_ζ^0 , is constant in the radial direction starting from the contact interface and ending at the external surface. This means that the axial displacement of the structure is entirely determined by the axial displacement at the external interface. In our case we have taken the external boundary condition on the axial displacement to be zero, see (26), and so this implies that

$$\tilde{u}_\zeta^0 = 0$$

everywhere in the structure. This is an interesting result since, often in the hemodynamics literature, the assumption that the axial displacement of the fluid-structure interface is zero, is imposed a priori. Here we showed that this is a reasonable assumption only if the external lateral boundary conditions are such that the axial component of the displacement at Σ_{ext} is zero. We state this results as a proposition.

Proposition 1. *Consider axially symmetric flow through a cylindrical tube with small aspect ratio $\epsilon = R/L$ and with three-dimensional linearly elastic walls of thickness h . Assume that the thickness h is comparable to the inner radius R of the tube, and allow the axial and longitudinal displacements of the wall structure to be of the same order of magnitude. Then, the leading-order axial displacement \tilde{u}_ζ^0 of the three-dimensional structure is entirely determined by the axial displacement of the structure's external boundary, namely, by the external lateral boundary condition.*

As a consequence, we have the following

Corollary 1. *The axial coordinates in both the Lagrangian and the Eulerian framework are identical to $O(\epsilon^2)$, namely,*

$$\tilde{z} = \tilde{\zeta} + \epsilon\tilde{u}_\zeta^0 + O(\epsilon^2) = \tilde{\zeta} + O(\epsilon^2). \quad (106)$$

With this property, the fluid-solid interface leading-order approximations are given by

$$\tilde{\gamma}^0(\tilde{\zeta}) = 1 + \frac{\delta}{R}\tilde{u}_s^0(1, \tilde{\zeta}) \quad \text{and} \quad \tilde{\gamma}^1(\tilde{\zeta}) = \frac{\delta}{R}\tilde{u}_s^1(1, \tilde{\zeta}). \quad (107)$$

Notice that they do not depend on the axial displacement to the ϵ^2 -accuracy!

We continue our calculation by determining the radial displacement \tilde{u}_s^0 . For this purpose we need to take into account the structure equation (86), the fluid-solid interface boundary condition (102) and the external boundary condition (25) describing the external pressure load on the structure. These two conditions provide the two boundary conditions for the second-order differential equation (86) determining \tilde{u}_s^0 :

$$\frac{\partial}{\partial\tilde{s}} \left[\frac{1}{\tilde{s}} \frac{\partial}{\partial\tilde{s}} (\tilde{s}\tilde{u}_s^0) \right] = 0, \quad \tilde{s} \in (1, 1 + h/R), \quad \tilde{\zeta} \in (0, 1), \quad (108)$$

$$\left(2 + \frac{\lambda_w}{\mu_w} \right) \frac{\partial\tilde{u}_s^0}{\partial\tilde{s}} + \frac{\lambda_w}{\mu_w} \frac{\tilde{u}_s^0}{\tilde{s}} = -\frac{PR}{\delta\mu_w} \tilde{\gamma}^0(\tilde{z}) \tilde{p}^0(\tilde{z}) \quad \text{at } \tilde{s} = 1, \quad (109)$$

$$\left(2 + \frac{\lambda_w}{\mu_w} \right) \frac{\partial\tilde{u}_s^0}{\partial\tilde{s}} + \frac{\lambda_w}{\mu_w} \frac{\tilde{u}_s^0}{\tilde{s}} = -\frac{PR}{\delta\mu_w} \tilde{P}_e \quad \text{at } \tilde{s} = 1 + h/R, \quad (110)$$

where $\tilde{\gamma}^0$ is given by equation (107). Here $\tilde{P}_e = P_e/P$ is the non-dimensional external pressure and $\tilde{\gamma}^0(\tilde{z})\tilde{p}^0(\tilde{z}) = \tilde{\gamma}^0(\tilde{\zeta})\tilde{p}^0(\tilde{\zeta})$ to the leading order. Notice that $\tilde{\zeta}$ here plays the role of a parameter since the differential operator involves only the radial variable \tilde{s} . The solution of problem (108)-(110) is simple:

$$\tilde{u}_s^0(\tilde{s}, \tilde{\zeta}) = [a_1\tilde{\gamma}^0(\tilde{z})\tilde{p}^0(\tilde{z}) - a_2\tilde{P}_e]\tilde{s} + [\tilde{\gamma}^0(\tilde{z})\tilde{p}^0(\tilde{z}) - \tilde{P}_e]\frac{a_3}{\tilde{s}}, \quad (111)$$

with constants a_1 , a_2 and a_3 given by:

$$a_1 = \frac{PR}{\delta\mu_w} \left[\frac{2h}{R} \left(2 + \frac{h}{R} \right) \left(1 + \frac{\lambda_w}{\mu_w} \right) \right]^{-1}, \quad a_2 = a_1 \left[1 + \frac{h}{R} \right]^2, \quad a_3 = a_1 \left[1 + \frac{\lambda_w}{\mu_w} \right] \left[1 + \frac{h}{R} \right]^2. \quad (112)$$

We can now use the expression for \tilde{u}_s^0 to express the leading-order fluid-solid interface entirely in terms of the internal (fluid) pressure and the external ambient pressure data. Namely, evaluating (111) at $\tilde{s} = 1$ and substituting it in (91) we obtain that

$$\tilde{\gamma}^0(\tilde{z}) = \frac{1 - b_1\tilde{P}_e}{1 - b_2\tilde{p}^0(\tilde{z})}, \quad (113)$$

where

$$b_1 = \frac{\delta}{R}(a_2 + a_3), \quad b_2 = \frac{\delta}{R}(a_1 + a_3). \quad (114)$$

With this equation we have obtained a closed system of equations that allows us to calculate the leading-order components of the fluid velocity $\tilde{v}_z^0, \tilde{v}_r^0$, the pressure \tilde{p}^0 , the fluid-structure interface $\tilde{\gamma}^0$, and the structure displacements $\tilde{u}_\zeta^0, \tilde{u}_s^0$. Recall that the fluid velocity and the structure displacement have been expressed in terms of \tilde{p}^0 and $\tilde{\gamma}^0$, see (94), (96) and (111). Thus, solving the two equations (99), (113) for \tilde{p}^0 and $\tilde{\gamma}^0$ will determine the leading-order solution to the fluid-structure interaction for the stationary Stokes flow. Substituting (113) into (99) and integrating (99) in \tilde{z} we get

$$\tilde{p}^0(\tilde{z}) = \frac{1}{b_2} \left[1 - (C_0\tilde{z} + C_1)^{-1/3} \right], \quad \tilde{z} \in (0, 1), \quad (115)$$

where C_0 and C_1 are constants determined by the inlet and outlet pressure data (42)

$$C_0 = \left[(1 - b_2\tilde{P}_L)^{-3} - (1 - b_2\tilde{P}_0)^{-3} \right], \quad C_1 = (1 - b_2\tilde{P}_0)^{-3}, \quad (116)$$

where \tilde{P}_0 and \tilde{P}_L are the non-dimensional inlet and outlet pressure data

$$\tilde{p}^0(0) = \tilde{P}_0, \quad \tilde{p}^0(1) = \tilde{P}_L. \quad (117)$$

This completes the calculation of the ϵ^0 -order solution to the fluid-structure interaction problem for the stationary Stokes flow. The solution is given by:

$$\boxed{\begin{aligned} \tilde{p}^0(\tilde{z}) &= \frac{1}{b_2} \left[1 - (C_0\tilde{z} + C_1)^{-1/3} \right], \\ \tilde{\gamma}^0(\tilde{z}) &= \frac{1 - b_1\tilde{P}_e}{1 - b_2\tilde{p}^0(\tilde{z})} = (1 - b_1\tilde{P}_e) (C_0\tilde{z} + C_1)^{1/3} \end{aligned} \quad \text{for } \tilde{z} \in (0, 1)}$$

PRESSURE AND THE FLUID-STRUCTURE INTERFACE

$$\boxed{\begin{aligned} \tilde{u}_s^0(\tilde{s}, \tilde{\zeta}) &= [a_1\tilde{\gamma}^0(\tilde{z})\tilde{p}^0(\tilde{z}) - a_2\tilde{P}_e]\tilde{s} + [\tilde{\gamma}^0(\tilde{z})\tilde{p}^0(\tilde{z}) - \tilde{P}_e]\frac{a_3}{\tilde{s}} \\ \tilde{u}_\zeta^0(\tilde{s}, \tilde{\zeta}) &= 0, \quad \text{for } \tilde{s} \in (1, 1 + \frac{h}{R}), \quad \tilde{\zeta} \in (0, 1). \end{aligned}}$$

RADIAL AND AXIAL DISPLACEMENT IN THE 3D STRUCTURE
where \tilde{z} and $\tilde{\zeta}$ are related via (93), and

$$\begin{aligned} \tilde{v}_z^0(\tilde{r}, \tilde{z}) &= \frac{1}{4}[\tilde{r}^2 - (\tilde{\gamma}^0(\tilde{z}))^2] \frac{d\tilde{p}^0}{d\tilde{z}}(\tilde{z}), \quad \tilde{r} \in (0, \tilde{\gamma}^0(\tilde{z})), \tilde{z} \in (0, 1) \\ \tilde{v}_r^0(\tilde{r}, \tilde{z}) &= 0, \end{aligned}$$

AXIAL AND RADIAL COMPONENT OF THE FLUID VELOCITY

where C_0 and C_1 are constants determined by (116), b_1 and b_2 are given by (114) and a_1, a_2 and a_3 given by (112).

6. The 1st-order correction. To calculate the ϵ -correction we proceed as before. First, we consider the boundary value problem for the ϵ -correction of the displacement \tilde{u}_s^1 . The problem is defined by the PDE (88), the fluid-structure interface boundary condition given by (104) and the external boundary condition (25), with $\tilde{u}_\zeta^0 = 0$:

$$\frac{\partial}{\partial \tilde{s}} \left[\frac{1}{\tilde{s}} \frac{\partial}{\partial \tilde{s}} (\tilde{s} \tilde{u}_s^1) \right] = 0, \quad \tilde{s} \in (1, 1 + h/R), \tilde{\zeta} \in (0, 1) \quad (118)$$

$$\left(2 + \frac{\lambda_w}{\mu_w} \right) \frac{\partial \tilde{u}_s^1}{\partial \tilde{s}} + \left(\frac{\lambda_w}{\mu_w} + \frac{P\tilde{p}^0(\tilde{z})}{\mu_w} \right) \frac{\tilde{u}_s^1}{\tilde{s}} = -\frac{PR}{\delta\mu_w} \tilde{\gamma}^0(\tilde{z}) \tilde{p}^1(\tilde{z}) \quad \text{at } \tilde{s} = 1, \quad (119)$$

$$\left(2 + \frac{\lambda_w}{\mu_w} \right) \frac{\partial \tilde{u}_s^1}{\partial \tilde{s}} + \frac{\lambda_w}{\mu_w} \frac{\tilde{u}_s^1}{\tilde{s}} = 0 \quad \text{at } \tilde{s} = 1 + h/R. \quad (120)$$

This system determines \tilde{u}_s^1 in terms of \tilde{p}^1 and the lower-order terms. Now, \tilde{u}_s^1 and \tilde{p}^1 are also related through equation (100). Thus, these two completely determine \tilde{u}_s^1 and \tilde{p}^1 in terms of the already calculated lower order approximations. With the \tilde{u}_s^1 and \tilde{p}^1 known, we can recover \tilde{v}_z^1 using (95). Therefore, the ϵ -corrections $\tilde{v}_z^1, \tilde{p}^1, \tilde{\gamma}^1, \tilde{u}_s^1$ can be easily determined from this closed system of equations. Notice that \tilde{u}_ζ^1 does not influence the calculation of these functions. The ϵ -correction of the axial displacement can be now determined by solving equation (89) with the boundary conditions (105) at the fluid-structure interface, and $\tilde{u}_\zeta^1 = 0$ at the external interface. Thus, the problem for \tilde{u}_ζ^1 reads:

$$\begin{aligned} \left(1 + \frac{3\tau}{4\mu_w} \tilde{T}_{ss} - \frac{\tau}{4\mu_w} \tilde{T}_{\zeta\zeta} \right) \frac{\partial \tilde{u}_\zeta^1}{\partial \tilde{s}} &= \frac{C_1(\tilde{\zeta})}{\tilde{s}} - \left[\left(1 + \frac{\lambda_w}{\mu_w} \right) - \frac{\tau}{4\mu_w} (\tilde{T}_{\zeta\zeta} + \tilde{T}_{ss}) \right] \frac{\partial \tilde{u}_s^0}{\partial \tilde{\zeta}}, \\ \frac{\delta\mu_w}{PR} \left(1 - \frac{\tau}{4\mu_w} \tilde{T}_{\zeta\zeta} \right) \frac{\partial \tilde{u}_\zeta^1}{\partial \tilde{s}} &= -\frac{\delta\mu_w}{PR} \left(1 - \frac{\tau}{4\mu_w} \tilde{T}_{\zeta\zeta} \right) \frac{\partial \tilde{u}_s^0}{\partial \tilde{\zeta}} \\ &\quad + \left\{ \frac{\partial \tilde{v}_z^0}{\partial \tilde{r}} + \frac{\delta}{R} \tilde{p}^0 \frac{\partial \tilde{u}_s^0}{\partial \tilde{\zeta}} \right\} \left(1 + \frac{\delta}{R} \frac{\tilde{u}_s^0}{\tilde{s}} \right) \quad \text{at } \tilde{s} = 1, \\ \tilde{u}_\zeta^1 &= 0 \quad \text{at } \tilde{s} = 1 + h/R. \end{aligned}$$

Notice that this is the only place where the pre-stress enters the calculation of the solution to this problem.

In addition, we have already calculated the ϵ -correction for the radial component of the velocity which is given by

$$\tilde{v}_r^1(\tilde{r}, \tilde{z}) = \frac{\tilde{r}}{4} \tilde{\gamma}^0 \frac{d\tilde{\gamma}^0}{d\tilde{z}} \frac{d\tilde{p}^0}{d\tilde{z}} - \frac{\tilde{r}^3}{16} \frac{d^2\tilde{p}^0}{d\tilde{z}^2} + \frac{\tilde{r}}{8} (\tilde{\gamma}^0)^2 \frac{d^2\tilde{p}^0}{d\tilde{z}^2}, \quad \tilde{r} \in (0, \tilde{\gamma}^0(\tilde{z})), \tilde{z} \in (0, 1). \quad (121)$$

We now have the following result.

Proposition 2. *The velocity field $\mathbf{v} = V_z(\tilde{v}_z^0 + \epsilon\tilde{v}_z^1, \epsilon\tilde{v}_r^1)$, the pressure $p = \frac{\mu V_z L}{R^2}(\tilde{p}^0 + \epsilon\tilde{p}^1)$, and the displacement $\mathbf{u} = \delta(\epsilon\tilde{u}_\zeta^1, \tilde{u}_s^0 + \epsilon\tilde{u}_s^1)$ solve problem (43)-(57) to the ϵ^2 -accuracy.*

The proof of this result follows the same steps and the proof of Proposition 7.1 in [7].

7. The pressure-radius relationship for a thick-walled cylinder with small deformations. In this section we derive an explicit pressure-radius relationship that holds for a pre-stressed, three-dimensional elastic tube, loaded by the pressure exerted by the stationary Stokes flow, under the assumption that the deformation of the structure is small. This will give rise to a generalization of the Law of Laplace that holds for thin elastic structures. We start by utilizing equations (113) and (91) to obtain

$$\frac{1 - b_1 \tilde{P}_e}{1 - b_2 \tilde{p}^0(\tilde{z})} = 1 + \frac{\delta}{R} \tilde{u}_s^0 \Big|_{\tilde{s}=1}. \quad (122)$$

We can write this equation in terms of the transmural pressure $\Delta\tilde{p}(\tilde{z})$ defined by

$$\Delta\tilde{p}(\tilde{z}) := \frac{b_2}{b_1} \tilde{p}^0(\tilde{z}) - \tilde{P}_e. \quad (123)$$

By noticing that $b_2 = b_1 + O(h/R)$, we see that in the case of a thin-walled cylinder, the definition of the transmural pressure (123) becomes the usual one, to the leading order:

$$\Delta\tilde{p}(\tilde{z}) := \tilde{p}^0(\tilde{z}) - \tilde{P}_e. \quad (124)$$

Now, the pressure-displacement relationship (122) becomes

$$\frac{1}{1 - \frac{b_1}{1 - b_1 \tilde{P}_e} \Delta\tilde{p}} = 1 + \frac{\delta}{R} \tilde{u}_s^0 \Big|_{\tilde{s}=1}. \quad (125)$$

Since our model was obtained by assuming linear theory of elasticity, it is meaningful to investigate the behavior of expression (113) for small transmural pressures $\Delta\tilde{p}$ which implies small deformation $\delta\tilde{u}_s$. By expanding equation (125) with respect to δ/R and ignoring the terms of order $(\delta/R)^2$ and smaller, one obtains the following leading-order pressure-displacement relationship, for a thick-walled cylinder with small deformations, written in dimensional form:

$$\Delta p(z) = \left(\frac{h}{R^2} \frac{2 + h/R}{(1 + h/R)^2} \frac{2\mu_w(\mu_w + \lambda_w)}{2\mu_w + \lambda_w} - \frac{P_e}{R} \right) u_s^0(R, z). \quad (126)$$

We can express the coefficients involving the Lamé constants λ_w and μ_w in terms of the Young's modulus E and the Poisson ratio σ by using

$$4\mu_w \frac{\lambda_w + \mu_w}{\lambda_w + 2\mu_w} = \frac{E}{1 - \sigma^2}, \quad \frac{2\mu_w \lambda_w}{\lambda_w + 2\mu_w} = \frac{E\sigma}{1 - \sigma^2}.$$

Then, the leading-order pressure-displacement relationship for a three-dimensional linearly elastic tube with wall thickness comparable to the tube radius, loaded by the stationary Stoke's flow, becomes

$$\boxed{\Delta p(z) = \left(K \frac{Eh}{(1 - \sigma^2)R^2} - \frac{P_e}{R} \right) u_s^0(R, z).} \quad (127)$$

where

$$K = \frac{1}{2} \frac{2 + h/R}{(1 + h/R)^2},$$

$u_s^0(R, z)$ is the radial displacement at the interface, and $\Delta p(z)$ is the transmural pressure, defined by (123). Notice that for $K = 1$ this is exactly the Law of Laplace. Indeed, by assuming that the cylinder wall is thin in the sense that $(h/R)^2$ is negligible, and by assuming small displacements, equation (127) reduces to the well-known Law of Laplace, describing a pre-stressed linearly elastic membrane shell, see e.g. equation (2.5) in [1]. Namely, we obtain

$$\Delta p(z) = \left(\frac{Eh}{(1 - \sigma^2)R^2} - \frac{P_e}{R} \right) u_s^0(R, z). \quad (128)$$

PARAMETERS	AORTA/ILIACS
Inner char. radius $R(m)$	0.003-0.012 [24]
Char. length $L(m)$	0.065-0.2 [10]
Dyn. viscosity $\mu_F(\frac{kg}{m \cdot s})$	3.5×10^{-3} [24]
Young's modulus $E(Pa)$	$10^9 - 10^6$ [24, 12, 14]

TABLE 2. Table with parameter values

The Law of Laplace has been widely used to model linearly elastic behavior of arterial walls in the blood flow literature, [4, 6, 10, 15, 21, 22, 24]. However, the thickness of the vessel walls in elastic and muscular arteries is very much comparable with the vessel radius, see Table 7, [20]. Thus, equation (127) is more appropriate as

ARTERY	RADIUS	WALL THICKNESS
ELASTIC ARTERY	9mm	1mm
MUSCULAR ARTERY	3mm	1mm

TABLE 3. Table with Radius and Wall Thickness Values

a model for the linearly elastic behavior of arterial walls. A calculation of the value of constant K for the muscular arteries is around 0.6, implying that the effective stiffness of the vessel wall with the new model is 0.6 of that in the Laplace Law. Similarly, a calculation of K corresponding to the elastic arteries is around 0.85 giving rise to an error of 0.15 which is larger than ϵ if L is larger than $6cm$, which is the case for the typical abdominal aorta. Thus, we conclude that using equation (127) instead of the Law of Laplace (128) is more appropriate for the blood flow application.

8. Numerically Calculated Solution. We conclude this manuscript by showing the numerically calculated solution emphasizing the structure deformation for a couple of different parameters. Figure 7 shows the radial and longitudinal displacement of the structure for the parameter values corresponding roughly to the blood flow application: the inlet pressure is taken to be $P_0 = 15990Pa$ which is about $120mmHg$, the outlet pressure $P_L = 14391Pa$, which is taken to be the same as the ambient pressure P_{ext} . The inner vessel radius $R = 3.1mm$ and the vessel wall thickness is $h = 0.9mm$. The vessel length is taken to be $L = 10cm$, and the Young's modulus of elasticity $E = 10^5Pa$. In both figures one can notice the "squeezing" of the structure near the inlet where the pressure difference between the ambient pressure and the lumen pressure (transmural pressure) is the highest, leading to the largest deformation. The two pictures in Figure 7 correspond to the incompressible

and a slightly compressible structure. We considered the case of a slightly compressible structure since it has been noted in [16] that arterial walls are not truly incompressible. The figure on the left shows the deformation for an incompressible structure with $\sigma = 0.5$ while the figure on the right shows the deformation for a slightly compressible structure with $\sigma = 0.49$. Both results have been calculated for the outlet pressure equal to the ambient pressure. Notice how the location of the fluid-structure interface differs in the two cases. In the incompressible case (left figure) the fluid-structure interface at the outlet boundary is not displaced, while in the compressible case, the displacement near the outlet is negative. This is in agreement with our calculation, in particular, with equation (113).

Remark. For a related numerical comparison of the solution to the reduced equations with the full 2D Finite Element Method calculations with different values of ϵ , please see [19]. Reference [19] discusses the flow through a long and narrow 2D pore in a porous medium with elastic walls. The pores were not pre-stressed, which considerably simplifies the calculations. However, similar ideas to those presented in this manuscript, were used in the derivation of the effective models in [19]. The focus of the work in [19] was on the *numerical* comparison between the reduced and the full model solutions, justifying the methodology used in the problem reduction. Excellent agreement was obtained.

Acknowledgements. Partial research support for the first author was provided by the NSF/NIGMS grant number DMS-0443826. Partial research support for the second author was provided by the Texas Higher Education Board under ARP grant number 003652-0051-2006. Partial research support for the third author was provided by NSF under grant number DMS-0245513, NSF/NIGMS grant number DMS-0443826, and by the Texas Higher Education Board under ARP grant number 003652-0051-2006. The authors would also like to thank Raffaella Rizzoni and Gianpetro Del Piero (Department of Engineering, University of Ferrara) for useful discussions.

REFERENCES

- [1] S. Čanić, J. Tambača, G. Guidoboni, A. Mikelić, C.J. Hartley, D. Rosenstrauch. *Modeling viscoelastic behavior of arterial walls and their interaction with pulsatile blood flow*. SIAM J Applied Mathematics. Volume 67(1) (2006) 164 -193.
- [2] A. Mikelić, G. Guidoboni, S. Čanić. *Fluid-Structure Interaction in a Pre-Stressed Tube with Thick Elastic Walls II: The Nonstationary Navier-Stokes Problem*. In preparation.
- [3] S. Čanić, J. Tambača, G. Guidoboni, A. Mikelić, C.J. Hartley, D. Rosenstrauch. *Blood Flow in Compliant Arteries: An Effective Viscoelastic Reduced Model, Numerics and Experimental Validation*. Annals Biomed. Eng. 34 (2006) 575-592 .
- [4] S. Čanić and E-H. Kim, *Mathematical analysis of the quasilinear effects in a hyperbolic model of blood flow through compliant axi-symmetric vessels*, Mathematical Methods in the Applied Sciences, 26(14) (2003), pp. 1161–1186.
- [5] S. Čanić and A. Mikelić, *Effective equations modeling the flow of a viscous incompressible fluid through a long elastic tube arising in the study of blood flow through small arteries.*, SIAM Journal on Applied Dynamical Systems, 2(3) (2003), pp. 431–463.
- [6] S. Čanić, A. Mikelić and J. Tambača *A two-dimensional effective model describing fluid-structure interaction in blood flow: analysis, simulation and experimental validation* Special Issue of Comptes Rendus Mechanique Acad. Sci. Paris (2005)
- [7] S. Čanić, A. Mikelić, D. Lamponi, and J. Tambača. *Self-Consistent Effective Equations Modeling Blood Flow in Medium-to-Large Compliant Arteries*. SIAM J. Multiscale Analysis and Simulation 3(3) (2005), pp. 559-596.
- [8] *Ultrasound of the Human Carotid Artery*. www.bmt.tue.nl/opleiding/ogo/0405/3eJaar/3.html.

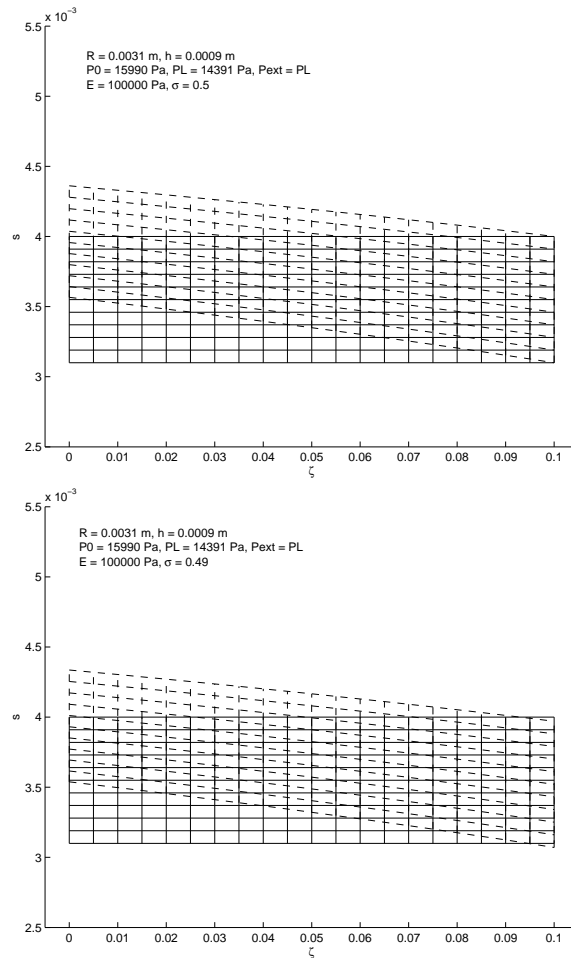


FIGURE 7. The figure shows a cross-section of a thick cylindrical structure along the length of the cylinder (fixed polar angle ϑ). The deformed structure is shown in dashed lines, while the reference configuration, which is pre-stressed but unloaded, is shown in solid lines. The figure on the left corresponds to the Poisson ratio $\sigma = 0.5$ (the incompressible case) and the figure on the right corresponds to the Poisson ratio $\sigma = 0.49$ (the almost incompressible case). Notice the negative displacement near the "outlet" of the almost incompressible structure.

- [9] H.C. Han, Y.C. Fung, *Direct measurement of transverse residual strains in aorta*, Am. J. Physiol. Heart Circ Physiol. **270** (1996) H750–H759
- [10] C. Chmielevsky, *"A Comparison of Two Models Predicting Blood Flow in the Systemic Arteries"*, M.S.Thesis, North Carolina State University (2004).
- [11] A. Delfino, N. Stergiopoulos, J. E. Moore, Jr and J.J. Meister, *Residual strain effect on the stress field in a thick wall finite element model of the human carotid bifurcation*, J. Biomechanics **30-8** (1997) 777–786

- [12] R. L. Armentano, J.G. Barra, J. Levenson, A. Simon, R.H. Pichel. *Arterial wall mechanics in conscious dogs: assessment of viscous, inertial, and elastic moduli to characterize aortic wall behavior*. Circ. Res. 76 (1995), pp. 468–478.
- [13] R. L. Armentano, J.L. Megnien, A. Simon, F. Bellenfant, J.G. Barra, J. Levenson. *Effects of hypertension on viscoelasticity of carotid and femoral arteries in humans*. Hypertension 26 (1995), pp. 48–54.
- [14] R. D. Bauer, R. Busse, A. Shabert, Y. Summa, E. Wetterer. *Separate determination of the pulsatile elastic and viscous forces developed in the arterial wall in vivo*. Pflugers Arch. 380 (1979), pp. 221–226.
- [15] Y.C. Fung, *Biomechanics: Circulation*, Springer, New York, 1993. Second Edition.
- [16] J. D. Humphrey, *Mechanics of the Arterial Wall: Review and Directions*, Critical Reviews in Biomedical Engineering Vol. 23 (1&2) 1995.
- [17] G.A. Holzapfel, T.C. Gasser, R.W. Ogden, *A new constitutive framework for arterial wall mechanics and a comparative study of material models*, J. Elasticity **61** (2000) 1–48
- [18] A. Hoger, *On the determination of residual stress in an elastic body*, J. Elasticity **16** (1986) 303–324
- [19] O. Iliev, A. Mikelić, P. Popov. *Fluid structure interaction problems in deformable porous media: Toward permeability of deformable porous media*. Preprint of Fraunhofer Institute in Kaiserslautern: Berichte des Fraunhofer ITWM, Nr. 65 (2004). Submitted to SIAM J Multiscale Modeling and Simulation. Under Revision.
- [20] E.N. Marieb, *Human Anatomy and Physiology* Sixth Edition. Pearson Benjamin Cummings, San Francisco 2004.
- [21] M. S. Olufsen, C. S. Peskin, W. Y. Kim, E. M. Pedersen, A. Nadim and J. Larsen, *Numerical Simulation and Experimental Validation of Blood Flow in Arteries with Structured-Tree Outflow Conditions*. Annals of Biomedical Engineering 28 (2000), pp. 1281–1299.
- [22] G. Pontrelli. *A mathematical model of flow through a viscoelastic tube*. Med. Biol. Eng. Comput, 2002.
- [23] A.M. Robertson and A. Sequeira, *A director theory approach to modeling blood flow in the arterial system: an alternative to classical 1D models*, M³ AS : Math. Models Methods Appl. Sci., Vol. 15 (no. 6) (2005), pp. 871–906.
- [24] A. Quarteroni, M. Tuveri and A. Veneziani, *Computational vascular fluid dynamics: problems, models and methods. Survey article*, Comput. Visual. Sci. 2 (2000), pp. 163–197.
- [25] Residual Stress. www.engin.umich.edu/.../bme332bloodves.htm.

Received September 15, 2004; revised February 2005.

E-mail address: Andro.Mikelic@univ-lyon1.fr; gio@math.uh.edu; canic@math.uh.edu